DYNAMIC STABILITY OF HYDRAULIC POPPET VALVES

by

Jens E. Jorgensen
S.B. Massachusetts Institute of Technology 1959

SUBMITTED IN PARTIAL FULFILLMENT

OF THE REQUIREMENTS FOR THE

DEGREE OF MASTER OF SCIENCE

AT THE

MASSACHUSETTS INSTITUTE OF TECHNOLOGY

May, 1963

Signature of Author: .....
Department of Mechanical Engineering,
May, 1963

Certified by: .....
Thesis Supervisor

Accepted by: .....
Chairman, Department Committee on
Graduate Students

DYNAMIC STABILITY OF HYDRAULIC POPPET VALVES

by

Jens E. Jorgensen

Submitted to the Department of Mechanical Engineering on May 17, 1963, in partial fulfillment of the requirements for the degree of Master of Science.

ABSTRACT

Stability criterion for a hydraulic poppet valve have been analysed and experimentally verified.

The analysis were based on the linearized equations. and on this basis a stability criterion for stable operation of a hydraulic poppet valve as a function of valve position and upstream geometry was formulated.

The validity of the equations developed were checked against an experimental model in the laboratory.

Thesis Supervisor: Shih-Ying Lee

Title: Associate Professor of Mechanical Engineering

ACKNOWLEDGMENTS

The author wishes to express his sincerest appreciation and indebtness to the following individuals for their contribution towards successful completion of this project:

Professor S.Y. Lee, thesis advisor, for introducing me to the problem and for his helpful guidance and constructive evaluations.

Mr. Kermit Harner for his sincere interest in the problem and constructive suggestions.

Mr. Karl Reid and all other members of the Engineering Projects Laboratory for valuable aid given whenever needed.

This thesis was supported in part by a Grant in Aid of the Hamilton Standard Division, United Aircraft Corporation and sponsored by the Engineering Projects Laboratory at Massachusetts Institute of Technology.

LIST OF ILLUSTRATIONS

List of Illustrations continued.

NOMENCLATURE

Symbol	Description and Unit
A	area, area of the line L (in^2)
C	coefficient of damping (lbs-sec/in)
D	diameter of line L and nozzle diameter (in)
F	poppet force (lbs)
f	valve frequency (cps)
G	valve pressure gain (lbs/in^3)
K	spring rate of external spring (lbs/in)
K_1	poppet flow sensitivity with displacement (in^2/sec)
K_2	poppet flow sensitivity with pressure (in^5/lbs-sec)
K_3	upstream orifice flow sensitivity with pressure (in^5/lbs-sec
K_4	poppet downstream flow sensitivity with pressure (in^5/lbs-sec)
K_5	downstream orifice flow sensitivity with pressure (in^5/lbs-sec)
L	length of line (in)
M	mass of poppet (lbs-sec^2/in)
P	fluid pressure, also pressure immediately upstream of the poppet valve
Q	flow rate through the poppet (in^3/sec)
T	time for wave to travel the length of line L (sec)
$\mathcal{V}_o$	system upstream volume (in^3)
	volume (in^3)
V	fluid velocity (in/sec)
X	valve displacement (in)

Nomenclature continued.

Symbol	Description and Unit
α	poppet cone half angle (degr.)
ϕ	phase lag between either pressure and force (degr.)
ρ	fluid density ($lbs\text{-}sec^2/in^4$)
β	fluid elasticity (psi)
ν	kinematic viscosity (in^3/sec)
$R = \frac{VD}{\nu}$	Reynolds no. (0)
$\delta = \frac{Av}{A}$	nondimensional valve displacement
$\gamma = \frac{Av}{Au}$	nondimensional valve displacement
τ	valve time constant (sec)
ω	valve frequency (rad/sec)
Δ	incremental change of a variable
$D = \frac{d}{dt}$	differential operator

Subscripts:

o	mean or time average condition of a variable
s	supply condition
v	valve - ref. to poppet valve
u	upstream condition
R	return condition
1 and 2	refers to sections 1 and 2 (adjacent)

TABLE OF CONTENTS

Table of Contents continued.

Table of Contents continued.

Part I Introduction, Conclusions and Recommendations

1.10 Introduction

A) Description

A poppet valve is a seating type valve where the valve member, poppet, has a relative motion perpendicular to its seat. A schematic of a poppet valve is shown in Figure 1-1. The design principle is simple in that the fluid forces on the poppet are balanced by an externally applied force, usually a spring force, and fluid is allowed to escape.

This type of device has extended use in high performance hydraulic systems as regulators, relief valves or hydraulic amplifiers.

Major advantages with the poppet type valve is its ease of manufacture, low leakage and insensitivity to dirt. The major problems arise in dynamic stability. The valve member itself is basically a mass spring system with little or no external damping and therefore oscillatory. Any additional fluid forces in phase with the valve velocity will lead to rapid unstable oscillations.

Oscillations of this type not only degrades the valve performance, but when sustained will destroy the valve.

The purpose of this investigation is to determine the cause of this instability and show limits of stable operation where they exist.

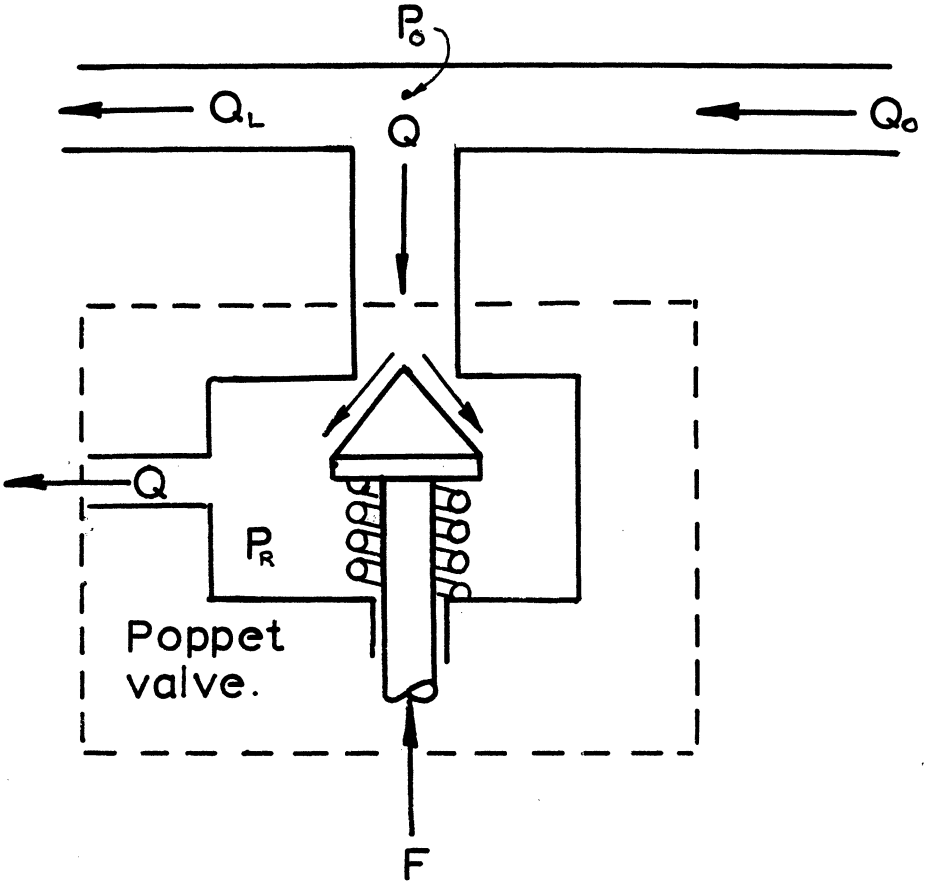

Q_o- Supply flow

Q_L- Load flow

Q - Relief or poppet flow

P_o- System pressure

POPPET VALVE.

FIGURE 1-1

B) Background

Previous investigation on stability of hydraulic valves has been done mostly on sliding and piston type valves.

Lee and Blackburn (Reference 1)[1] have shown that transient valve forces may cause instability. Static stability of poppet valves was investigated by Stone (Ref.#2) and dynamic studies on pneumatic flappertype valves have been carried out. (Ref.#3,4 and 5) Investigations by Ainsworth (Ref.#6) pointed out that the fluid delivery line interacts with a valve to cause instability, an investigation extended to the poppet valve by Funk (Ref.#7).

The result here is that the critical frequency in the system is the first harmonic of the delivery line higher than the natural frequency of the valve.

An interesting derivation by Frendenreich (Ref.#8) shows that a spring loaded relief valve regulating a constant flow is stabilized by the transient forces created due to the change in volume by the poppet motion, but will become unstable due to elasticity of the oil.

In this investigation the stability of the valve itself will studied, rather than stability due to interaction with other elements of a system as this is one step

[1] Number refers to list of references listed in Appendix E.

further removed.

Assumptions will been made as to the particular configuration to be studied, and an analysis will be made indicating the system characteristics and stability depending on the physical characteristics.

The model to be studied will include the effects of fluid inertia and compressibility, and compared with experimental results.

The analysis is presented in Part II and the experimental results in Part III of this thesis.

1.20 Conclusion

This investigation has lead to a better understanding of the basic problem of poppet valve stability.

The major fluid forces acting on the poppet valve are due to the fluid pressure. These pressure forces have components in the direction of the velocity and may stabilize or unstabilize the valve. It has been shown that the fluid elasticity contributes an unstabilizing force in the direction of the valve velocity and acts as a negative damping, where as the inertia forces associated with fluid acceleration have stabilizing components opposing the valve velocity and hence acts as positive damping.

The effect of fluid elasticity was by far the largest

factor in the cause of instability.

The stabilizing component due to inertia is also decreased due to frictional losses in the fluid flow.

The system analysis was made by linearizing the nonlinear differential equations and predictions were made with respect to system performance.

A limit for stable valve operation was derived and the experimental results verified the validity of the equations.

This study was only concerned with the condition upstream of the valve, but extension of the analysis to include the downstream effects are possible.

1.30 Recommendations

Based on this investigation the following recommendations are made. They are categorized in the two groups, Experimental and Design Analysis.

A. Experimental

Further data could be needed to extend the theory to some of the models not considered here.

A more important study can be made on the stability due to the downstream fluid momentum effects. Studies related to the pressure distribution and flow pattern around the poppet when confined in a narrow downstream

chamber will be important, and qualitative information is lacking.

B. Design Analysis

The nonlinear equations that describe this system can easily be studied on a analog computer. A study on the nonlinear characteristics could give more accurate information on valve stability, especially in the region of small valve openings or large disturbances.

A computer aided design would also reveal information not now available to the designer in the form of graphs and diagrams relating system stability and valve performance as function of the physical parameters.

Part II. Analysis

2.00 Introduction

The main task of this analysis is to conceive a meaningful mathematical model and define the problem. By breaking the system down into basic components and investigating each, it is hoped to gain insight to the nature of the stability.

The basic components are then combined and the overall system stability studied.

2.10 Model and System Description

A general schematic of the system is shown on Figure 2-1a. It is comprised of a constant upstream pressure

Ps, an upstream restriction Au, a delivery line L, and the system volume $\forall_o$ terminated by the poppet valve. The poppet valve is described by the motion $\underline{x}$ and its corresponding valve area A_V. The downstream conditions are assumed constant and in the analysis P_R is arbitrarily set to zero. The fluid is characterized by its density ρ and elasticity β (psi). A system of this nature can be looked upon as distributed or lumped parameter system.

The analysis here will based on the lumped parameter model as this will yield the most information.

The borderline between the two cases is approached when wave transmission due to valve motion becomes important. The time T for a wave to travel the distance L is given by

$$T = L\sqrt{\rho/\beta} \tag{1}$$

and the particular time constant for the system may be given as $\underline{t}$. Our criteria then becomes

$$\frac{T}{\tau} << 1 \tag{2}$$

and for a line it will be shown later that t

so that we have

$$\frac{\sqrt{\rho/\beta}\, Q_o}{A} \tag{3}$$

where A is the line area and Q_o is the mean flow. We assume here that equation (3) is valid. From earlier experiments (Ref.#9) it was established that the major fluid forces on the poppet were contributed by the pressure forces. The first task then becomes to calculate these pressure forces, and to make the analysis easier two basic models are first considered, and shown on Figure 2-1 b and c.

Compressible Model

Inertial effects are assumed negligible and the system is described by the orifice Au, the poppet valve Av s system volume $\mathcal{V}_o$ and the fluid propperties ρ and β .

Inertia Model

The volume $\mathcal{V}_o$ is assumed small and the fluid is incompressible. System is described by the line L, orifice, valve and the fluid density ρ .

The total system is then described by these combinations in a combined model later, which will be the representation of the system as shown on Figure 2-1a.

Before the actual analysis on the specific models are carried out, a general description of the forces and stability will be considered.

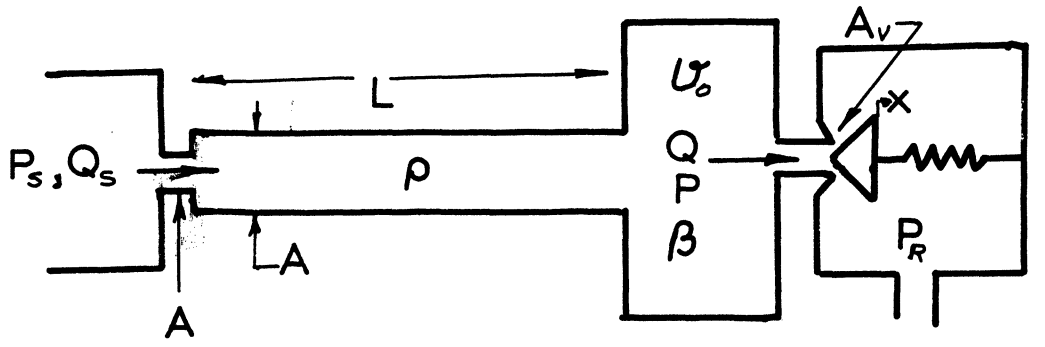

(A) General System Schematic.

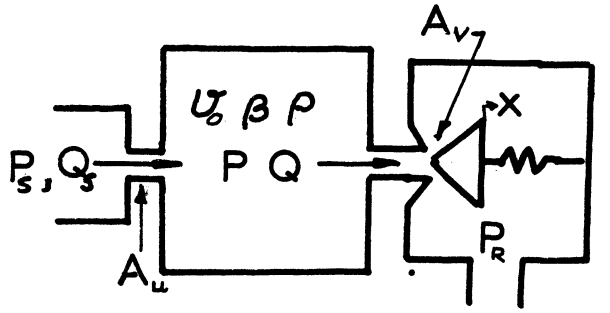

(B) Compressibility Model

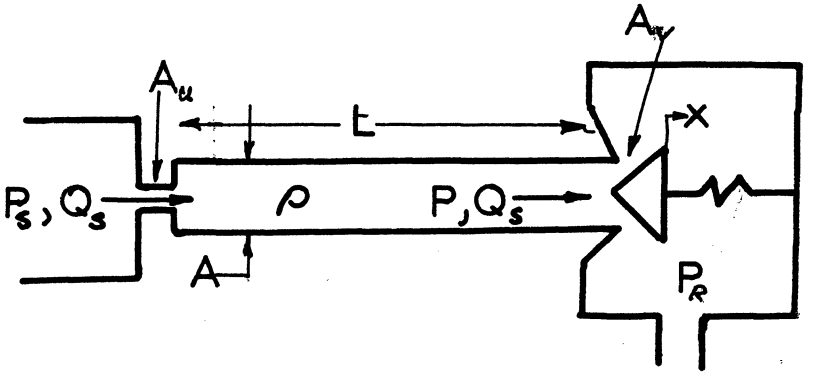

(C) Inertia Model

SYSTEM DESCRIPTION

Fig. 2-1

2.20 Static Characteristics and Stability

Evaluation of the static force is done by applying the momentum equation to the control volume shown on Figure 2-2.

$$(P_1 - P_2)A - F = \rho(V_2 A_v \sin\alpha)V_2 \cos\alpha - \rho V_1 A_1 \qquad (4)$$

Relating the velocities to the stagnation pressure and use continuity equation for the control volume gives:

$$F = P_o\{(1+\delta^2 \sin\alpha) - 2\delta \sin 2\alpha \qquad (5)$$

$$\delta \equiv \frac{A_v}{A} \qquad (6)$$

where the dimensionless valve displacement is defined only between

$$0 \leq \delta \leq 1 \qquad (7)$$

Two variations of equation (5) exist, if the system employs an upstream orifice or not.
Without an upstream orifice, $P_o = P_s$ and for a flat faced poppet $(\alpha = 0)$

$$F = P_s A(1-\delta^2) \qquad (8)$$

The static force is seen to increase with displacement, so the poppet must be restrained by an external spring of rate K.

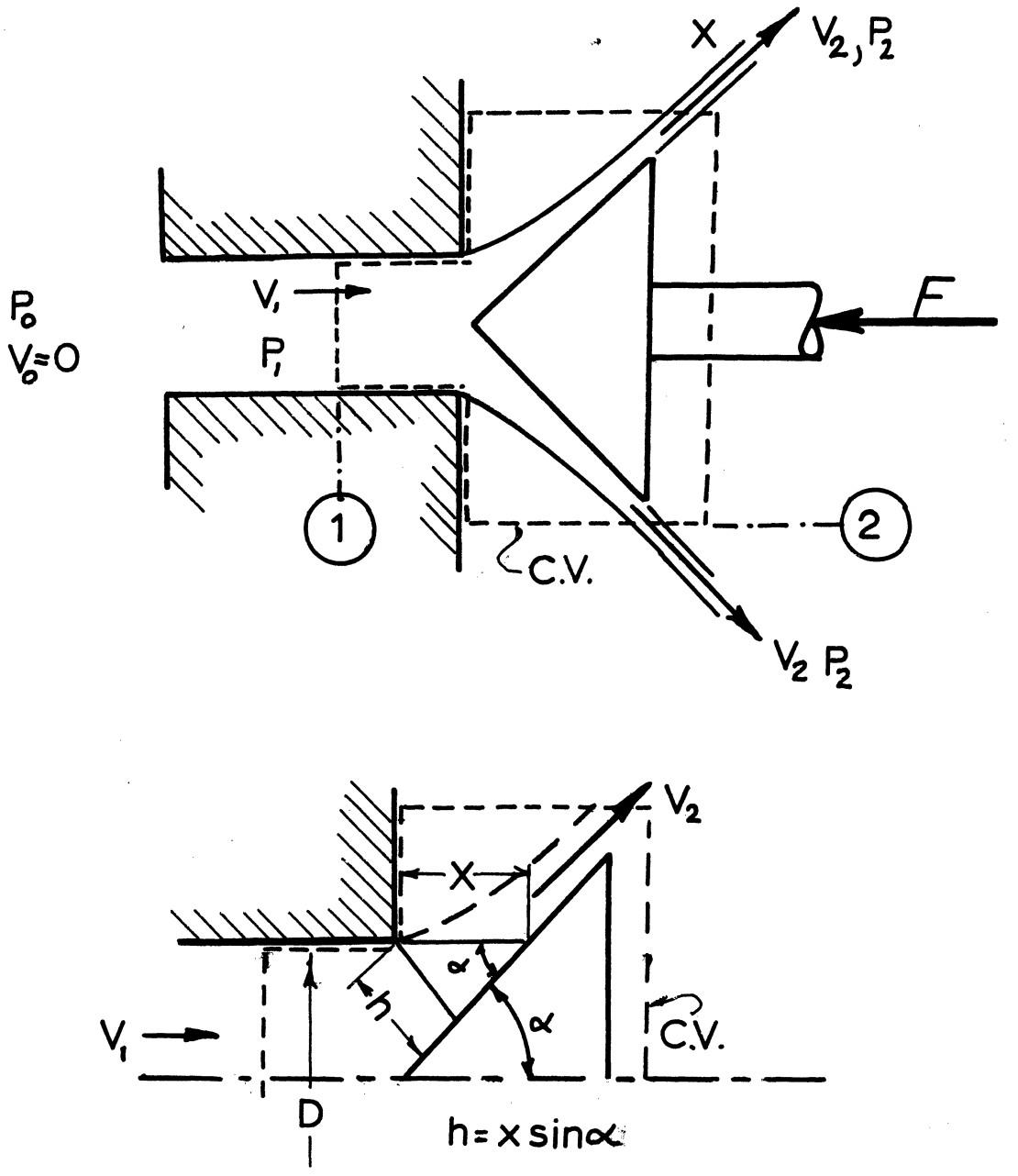

SYSTEM CONTROL VOLUME

FIGURE 2-2

$$K \gtrsim (2\pi D) P_s \delta \tag{9}$$

to ensure static stability.

For the case where the system have an upstream orfice of area Av the flow continuity gives

$$\frac{P}{P_s} = \frac{1}{1+\gamma^2} \tag{10}$$

where

$$\gamma \equiv \frac{A_v}{A_u} \tag{11}$$

Substituted into (5) for a flat faced poppet this gives

$$\frac{F}{F_o} = \frac{1}{1+\gamma^2} \tag{12}$$

where the assumption is made that $\delta^2 << \gamma^2$ and $F_o = P_s A$. This result is plotted on Figure 2-2. and since the force now decreases with displacement the system is statically stable and with a hydraulic spring rate

$$K_H = -(2\pi D) P_s \frac{\gamma}{(\gamma^2+1)} \tag{13}$$

Figure 2-3 also shows the response to a slow sinusoidal variation in the valve displacement.

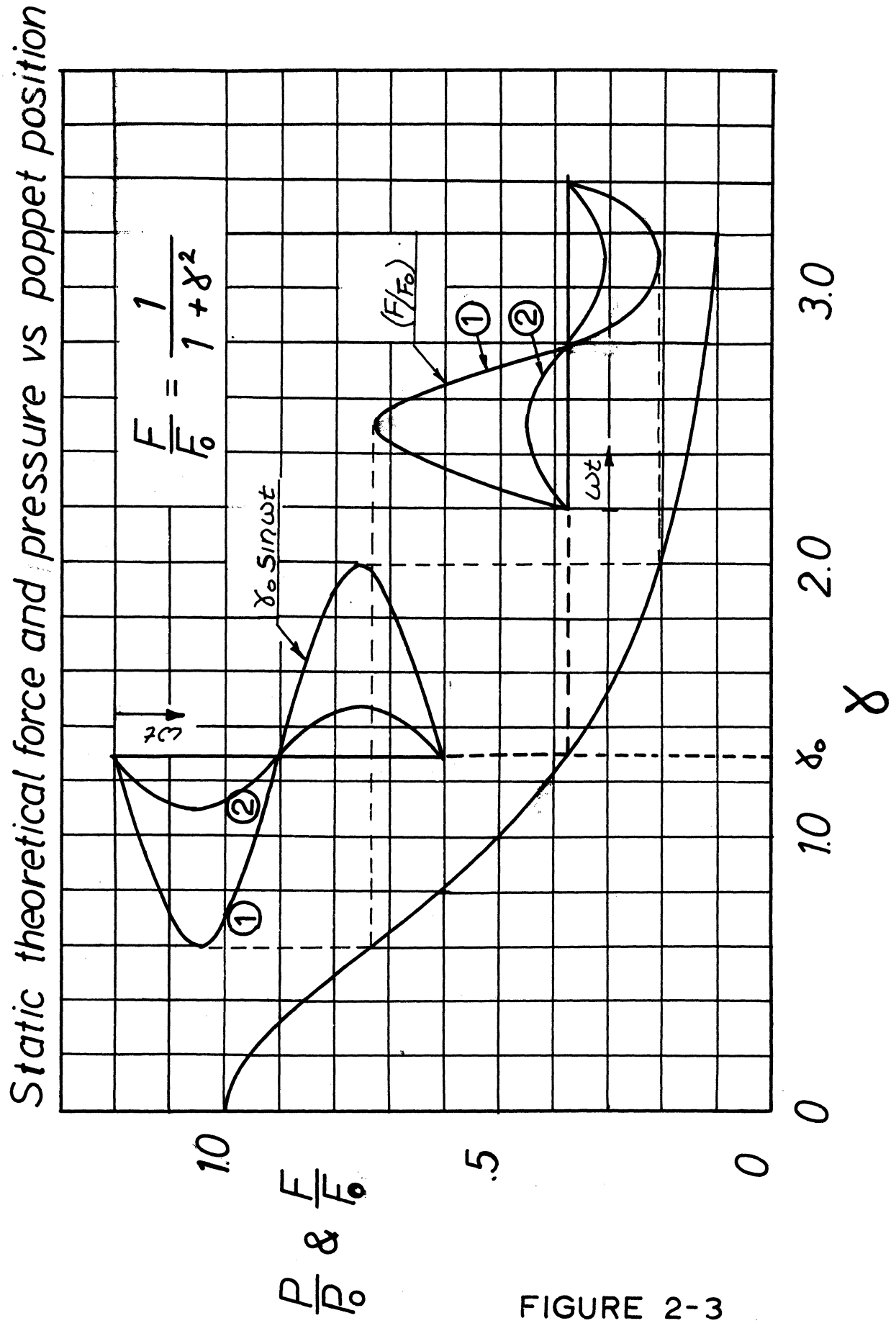
Static theoretical force and pressure vs poppet position
$\frac{F}{F_0} = \frac{1}{1+\gamma^2}$
(F/F_0)
$\gamma_0 \sin\omega t$
ωt
1
2
1.0
.5
0
1.0
2.0
3.0
γ_0
γ
F/F_0
&
P/P_0

FIGURE 2-3

The response is seen to depend not only on the operating displacement x_o but also on the amplitude of the valve. Large amplitude represented by curve (1) is seen to give a nonlinear output where as curve (2) gives a linear operation. Operation at small valve neutral position will also give nonlinear operation regardless of amplitude.

This analysis is most concerned with the linear operation because by linearizing the differential equations analytic solutions may be obtained, where as graphical or computer techniques must be employed in the nonlinear case.

2.30 Dynamic Stability

In this section a general presentation of system stability will be given. The system is assumed statically stable and the major consideration is given to linear operation.

2.31 Forces on the Poppet

The momentum equation used on the control volume in Figure 2-2 for the dynamic case yields:

$$(P_1 - P_2)A - F = \frac{d}{dt}(mV)_{cv} + \rho V^2 A_v \cos\alpha \sin\alpha - \rho V_1^2 A_1 \qquad (14)$$

Equation (14) as written assumes that Pr is constant everywhere downstream and fluid is carried across the boundary only by the fluid jet. This leaves out the complexity of the downstream flow pattern were turbulence and vorticity in general complicates the picture. Considering a flat poppet only and assuming that $V_1 << V_2$ the momentum equation leaves only pressure force and external force to balance the momentum change within the control volume. The poppet momentum is easily evaluated, but the momentum of the oil is more complicated. The assumption is made that this is small as previous experiments indicates this. (See Ref. #9 for detailed analysis). The momentum equation then reduces to the simple form if P_2 is constant and arbitrarily set to zero, and pressure immediately upstream of the valve is P

$$pA - F = M\ddot{x} \qquad (15)$$

M is the poppet mass and F the external force.

This then shows that the major fluid force is the pressure force acting on the poppet. The pressure P can be derived analytically or determined experimentally as functions of system parameters. Both methods are employed here.

2.32 General Stability Consideration

The force on the poppet is described by equation (15) which written for the system shown on Figure 2-4, yields

$$PA - F - C\dot{x} - Kx = M\ddot{x} \qquad (16)$$

In a linearized form where the motion x is given about some point xo we have

$$x = x_o + \Delta x$$

$$F = F_o + \Delta F$$

$$P = P_o + \Delta P \quad \text{where it is specified}$$

that $F_o = P_o A$ This gives

$$(\Delta P)A - Kx - C\dot{x} - M\ddot{x} - F = 0 \qquad (17)$$

This equation is shown in the vector diagram on Figure 2-4 for a free vibration (F = 0).

Let us look at the physics of the system first. With the fluid incompressible and inertia effects neglected the fluid pressure behind the poppet P is given by the instantaneous position of the poppet. For the free vibration this is shown on Figure 2-4 where x vibrates about x_o and the pressure varies about the mean pressure p_o, given by curve a, but opposite of the motion x, so it acts as a spring force. The net work done by the fluid pressure on the poppet is here zero, as when the poppet moves inward from

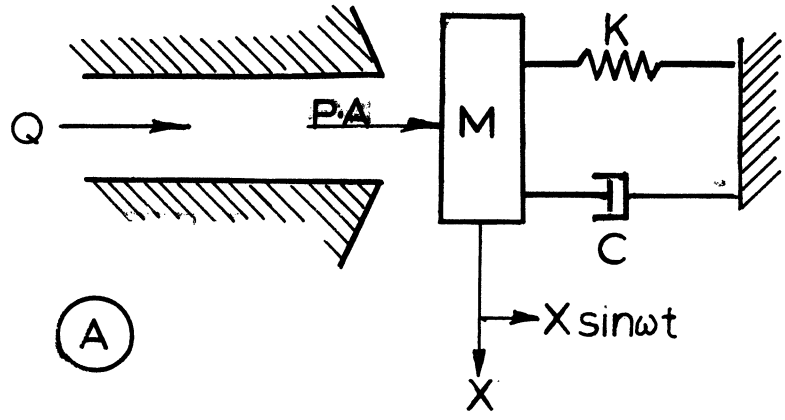

$$\Delta\left(\frac{P}{X}\right) = -G(j\omega)$$

$$(\Delta P)A - KX - C\dot{X} - M\ddot{X} = 0$$

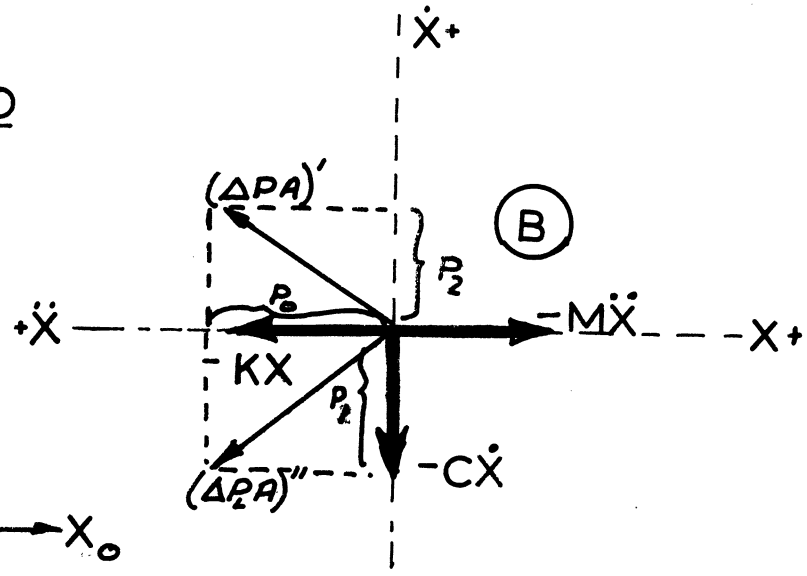

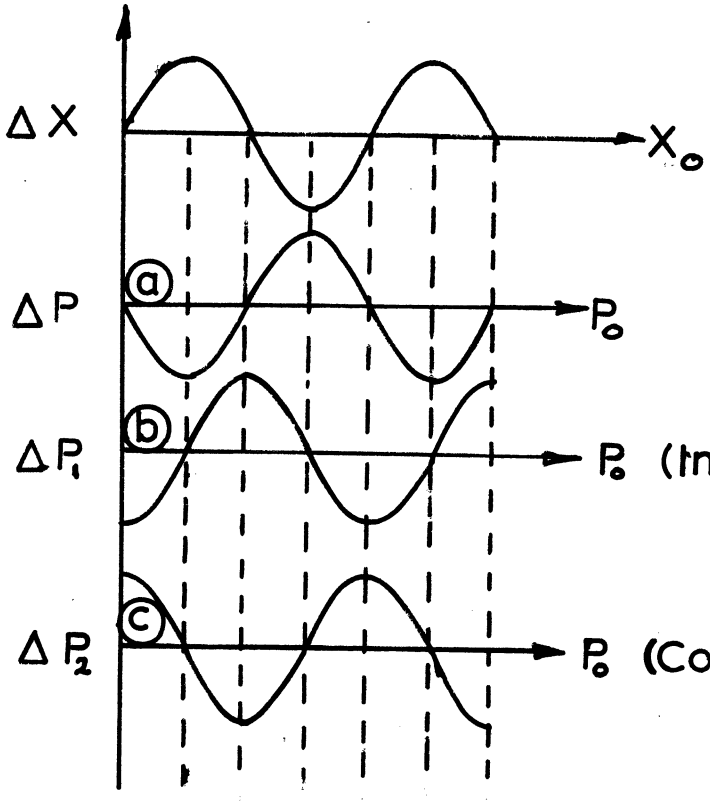

C

$$X = X_0 + \Delta X \sin\omega t$$

$$P = P_0 - \Delta P \sin\omega t$$

GENERALIZED SYSTEM RESPONSE

FIGURE 2-4

B to D the mean pressure in p_o and for the outward motion D - F the mean pressure is again p_o. The poppet neither gains nor loses energy from this component of pressure.

Consider first the effect of inertia, and use the super position principle, as the inertia effect will modify the existing pressure.

As the valve moves outwards, the flow increases and the resulting fluid acceleration further decreases the pressure. On the inward motion the flow decreases and the retardation of the flow increases the pressure further. This gives rise to the additional pressure p_1 shown in b (on Figure 2-4) which has its minimum at position A and maximum at c. The total pressure is now given by $p + p_1$ (shown vectorially as (P A)" on Figure 2-4) but as p does not contribute any net energy to the system, we need only consider p_1. When the poppet moves from B - D the mean pressure is greater than for the outward motion from B - F so that the net work done by the poppet is negative. The pressure p_1 depends on the velocity and opposes it, so it acts as a positive damping in that the fluid gains energy from the motion, and stabilizes it. The component in the direction of the velocity of (P A)' on Figure 2-4 is then p_1.

Next consider the effect of fluid compressibility only.

Again, this added storage capacity modifies the original pressure shown in a. As the poppet moves outward from A-C the flow exceeds the mean flow and the pressure steadily drops while on the inward motion the flow is less then the mean and the pressure rises. The additional pressure due to the compressibility p_2 has a minimum at c and maximum at A and E, so the total pressure is now $p + p_2$ (This is shown vectorially as (P A)' on Figure 2-4) Again we consider the work done by p_2 only. As the poppet moves from B - D now it sees a mean pressure less p_o and for the outward motion is larger than p_o so the net work done by the fluid on the is positive. Again the pressure p_2 depends on and is in the direction of the velocity. This is an unstable vibration, as once started the fluid pumps energy into the system and the vibration increases.

If the effects of compressibility and inertia are combined it depends on the vectorial sum of the three pressure forces if the resultant is to have a component in phase or out of phase with the velocity.

Mathematically this will be expressed by equation (17) combined with the equation for P = f(x) that will be developed later. Assume this function is of the form of a general differential equation

$$\Delta\left(\frac{P}{x}\right) = -G(D) \qquad (18)$$

Combined with equation (17) this gives

$$\Delta\left(\frac{F}{X}\right) = -\frac{1}{MD^2+CD+K+AG(D)} \tag{19}$$

which when examined for stability gives the frequency equation

$$[MD^2+CD+K+AG(D)]\,X = 0 \tag{20}$$

where $j\omega$ will be substituted for D.

Assume further that the general solution for G(D) is of the form:

$$G(D) = \frac{B_2D^2+B_1D+1}{A_2D^2+A_1D+1} \tag{21}$$

Substituted into 20 it gives a general fourth order vibration equation.

$$\{MA_2D^4+(MA_1+CA_2)D^3+(M+CA_1+KA_2+GAB_2)D + (C+KA_1+GAB_1)D+(K+GA)\}X = 0 \tag{22}$$

The stability of this equation is given by the Routh criteria (See Appendix B-3) and will be discussed in detail, as the various forms of G(D) are developed.

2.40 Compressibility

2.41 Dynamic Equation

In this section the analysis will be made of the adopted model by considering the elastic properties of the fluid. The system under consideration is shown in Figure (2-5a)

The system consists of an upstream orifice (Au), the volume $\mathcal{V}_o$, and poppet valve (A_v) and assumes p_S and p_R constant, density ρ and compressibility β.

System eqn's:

$$\rho(Q_s - Q) = \frac{\partial}{\partial t}(\mathcal{V}_o \rho) \tag{23}$$

$$Q_s = A_u \sqrt{\frac{2}{\rho}(P_s - P)} \tag{24}$$

$$Q = A_v \sqrt{\frac{2}{\rho}(P - P_R)} \tag{25}$$

$$\rho = \rho_o + \frac{\rho_o}{\beta} P \tag{26}$$

As is evident, these equations are nonlinear by the nature of the flow, so we are going to consider their linearized form.

We shall consider motions around a operating point x_o

of the poppet with corresponding flows and pressures given by

$$x = x_o + \Delta x$$

$$Q = Q_o + \Delta Q$$

$$p = p_o + \Delta p \text{ etc.}$$

The above operations then takes the form (Ref. Appendix B-1)

$$Q_s - Q = \frac{V_o}{\beta} DP \tag{27}$$

$$Q_s = -K_3 P \tag{28}$$

$$Q = K_1 X + K_2 P \tag{29}$$

where the variables now denote changes from the mean, and D is the linear differential operator d/dt and K_2 and K_3 are the flow sensitivity coefficients with respect to pressure and K_1 the flow sensitivity with respect to valve position.

These equations solved for p vs. x give

$$\Delta\left(\frac{P}{X}\right) = -\frac{K_1}{K_2+K_3}\left\{\frac{1}{\left[\frac{V_o}{\beta(K_2+K_3)}\right]D+1}\right\} \tag{30}$$

or:

$$\Delta\left(\frac{P}{X}\right) = \frac{G_c}{\tau_c D+1} \tag{31}$$

where

$$G_1 = \frac{K_1}{K_2 + K_3} \tag{32}$$

$$\tau_c = \frac{V_0}{\beta(K_3 + K_2)} \tag{33}$$

Equation (31) describes the desired pressure variation with poppet position, and as expected it is a simple lag with a time constant τ_0 proportional to the volume and inversely proportional to the fluid elasticity. By introducing the values for K_1, K_2 and K_3 as functions of geometry (Ref. Appendix B-1), we can further reduce equations (32) and (33) to:

$$G_1 = \frac{2P_s \pi D}{A_u}\left[\frac{\gamma}{\gamma^2+1}\right] \tag{34}$$

$$\tau_c = \frac{2V_0}{\beta A_u}\sqrt{\frac{\rho P_s}{2}}\left[\frac{\gamma}{(\gamma^2+1)^{3/2}}\right] \tag{35}$$

Introducing a system compliance z_c given by

$$Z_c = \frac{\beta A_u}{4\pi V_0}\sqrt{\frac{2}{\rho P_s}} \tag{36}$$

and the break frequency f_c given by the relations

$\omega \tau_c = 1$ and $\omega = 2\pi f$ so

$$f_c = \frac{1}{2\pi \tau_c}$$

we have for equation (35)

$$\Phi \equiv \frac{f_c}{Z_c} = \frac{(\gamma^2+1)^{3/2}}{\gamma} \tag{37}$$

and the function Φ plotted on Figure 2-6.

The minimum point for Φ is given by

$$\frac{d\Phi}{d\gamma} = 0$$

which gives

$$\Phi_{min} = 2.60$$

at $$\gamma = .707 \tag{38}$$

The point $\gamma = .707$ then represents the largest value of t_c and the minimum breakfrequency.

2.42 Stability

With the system transter function as given by (31) we have for the frequency equation (22):

$$\{M\tau_c D^3 + (M + C\tau_c)D^2 + (\tau_c K + C)D + (K + AG_1)\}x = 0 \tag{39}$$

First assume $C = 0$, and from Appendix B, equations B-36 and 37 give

$$G_1 > 0 \tag{40}$$

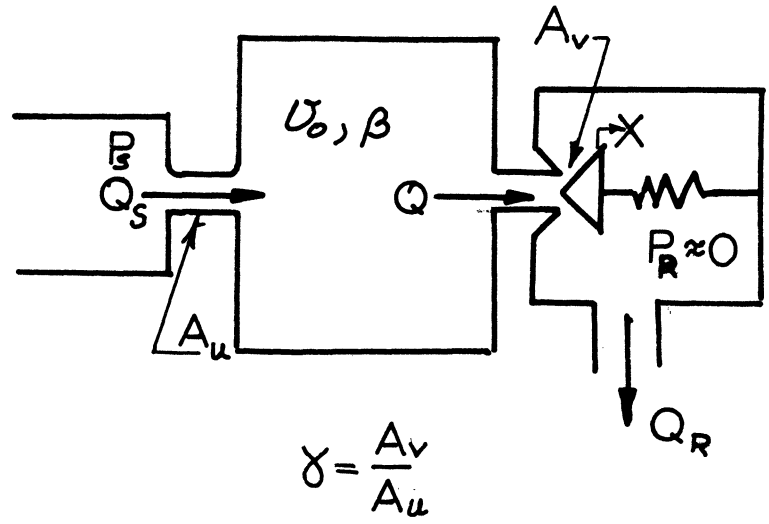

(A) COMPRESSIBILITY MODEL

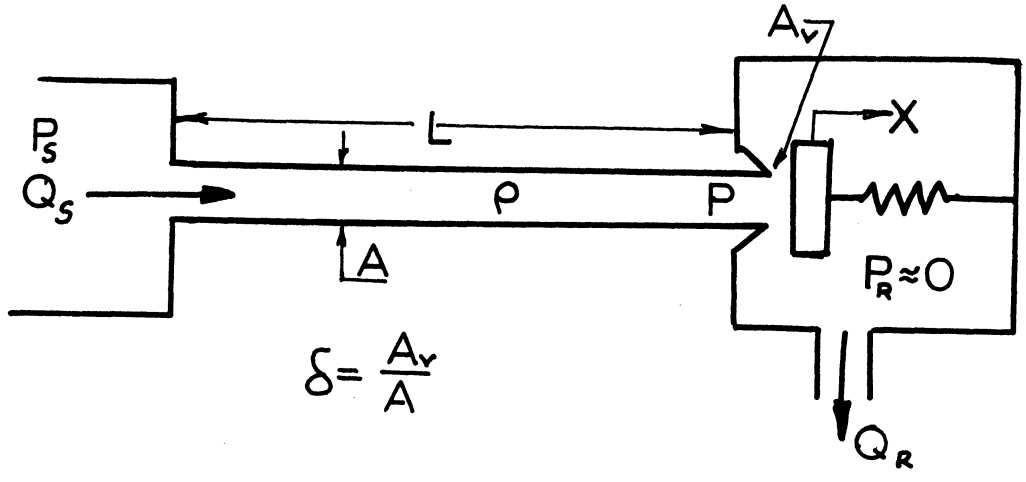

(B) INERTIA MODEL

SYSTEM MODELS

FIGURE 2-5

Dimensionless lag timeconstant vs poppet valve opening

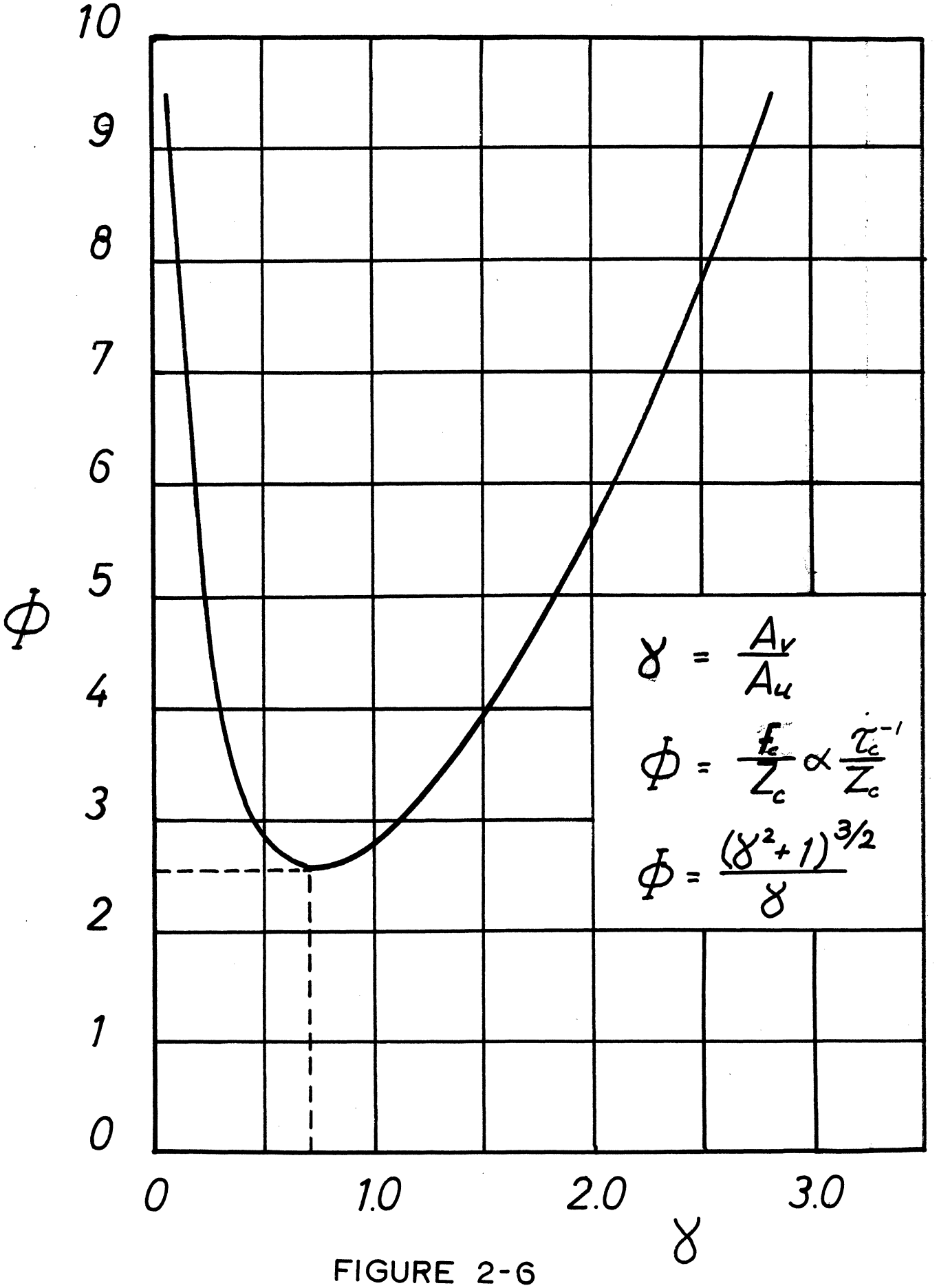

FIGURE 2-6

and $$\tau_c K M \geq M \tau_c (K + GA)$$ or

$$G_1 < 0$$

But the last statement contradicts the inequality given by equation (40), so we conclude that the system is unstable. This also agrees with the physical reasoning because the lag introduced gives a force component in the direction of velocity.

Necessary damping for system stability is given by (39) with K = 0 as

$$C \geqslant -\frac{M}{2\tau} \pm \sqrt{\left(\frac{M}{2\tau}\right)^2 + MAG} \qquad (41)$$

2.50 Inertia Model

2.51 Dynamical Equation

The fluid is here considered incompressible and with density ρ . The general system is shown in Figure 2-5 and consists of a constant pressure supply p_s and a line of length L and area A terminated by the poppet valve. Again we consider the linearized form:

System equations:

Line: $$P = -\left[\frac{\rho L}{A} D + \frac{\rho Q_0}{A^2}\right] Q_s \qquad (42)^*$$

*Ref. Appendix B-2

Valve: $$Q_s = K_1 x + K_2 P \tag{43}$$

Combine and solve for p

$$\Delta\left(\frac{P}{x}\right) = -\frac{\rho Q_0 K_1}{A^2 + \rho Q_0 K_2} \frac{\left(\frac{LA}{Q_0} D + 1\right)}{\left(\left[\frac{\rho L A K_2}{\rho Q_0 K_2 + A^2}\right] D + 1\right)} \tag{44}$$

which can be reduced to the form

$$\Delta\left(\frac{P}{x}\right) = -G_2 \frac{\tau_L D + 1}{\tau_2 D + 1} \tag{45}$$

where the guantities are defined by equation (44). Substitution for K_1, K_2 gives:

$$\tau_L = \frac{L}{\sqrt{\frac{2}{\rho} P_s}} \frac{1}{\delta} \tag{46}$$

$$\tau_2 = \frac{L}{\sqrt{\frac{2}{\rho} P_s}} \frac{\delta}{1+\delta^2} \tag{47}$$

and

$$\frac{\tau_L}{\tau_2} = 1 + \frac{1}{\delta^2} \tag{48}$$

These equations are plotted on Figure 2-7 and 2-8 in a nondimensional form.

The lead frequency τ_c is proportional to the line length and inversely proportional to the pressure and

valve opening δ .

The valve gain is given by

$$G_2 = \frac{2P_s \pi D}{A} \frac{\delta}{\delta^2+1} \tag{49}$$

For a system with an upstream orifice included, the calculations are the same and shown in Appendix C-1. The values for the time constant are changed by the ratio of the upstream to downstream area.

2.52 Stability

With G(D) given by equation (45) we have for the frequency equation (22) with $C = 0$, i.e., no external damping.

$$\{M\tau_2 D^3 + MD^2 + (K\tau_2 + GA\tau_L)D + (K+GA)\}x = 0 \tag{50}$$

Stability is again given by C-36 and 37 and gives

$$K + G_2 A > 0 \tag{51}$$

and $$M(\tau_2 K + AG_2\tau_L) > M\tau_2(AG+K)$$

which gives

$$\frac{\tau_L}{\tau_2} > 1 \tag{52}$$

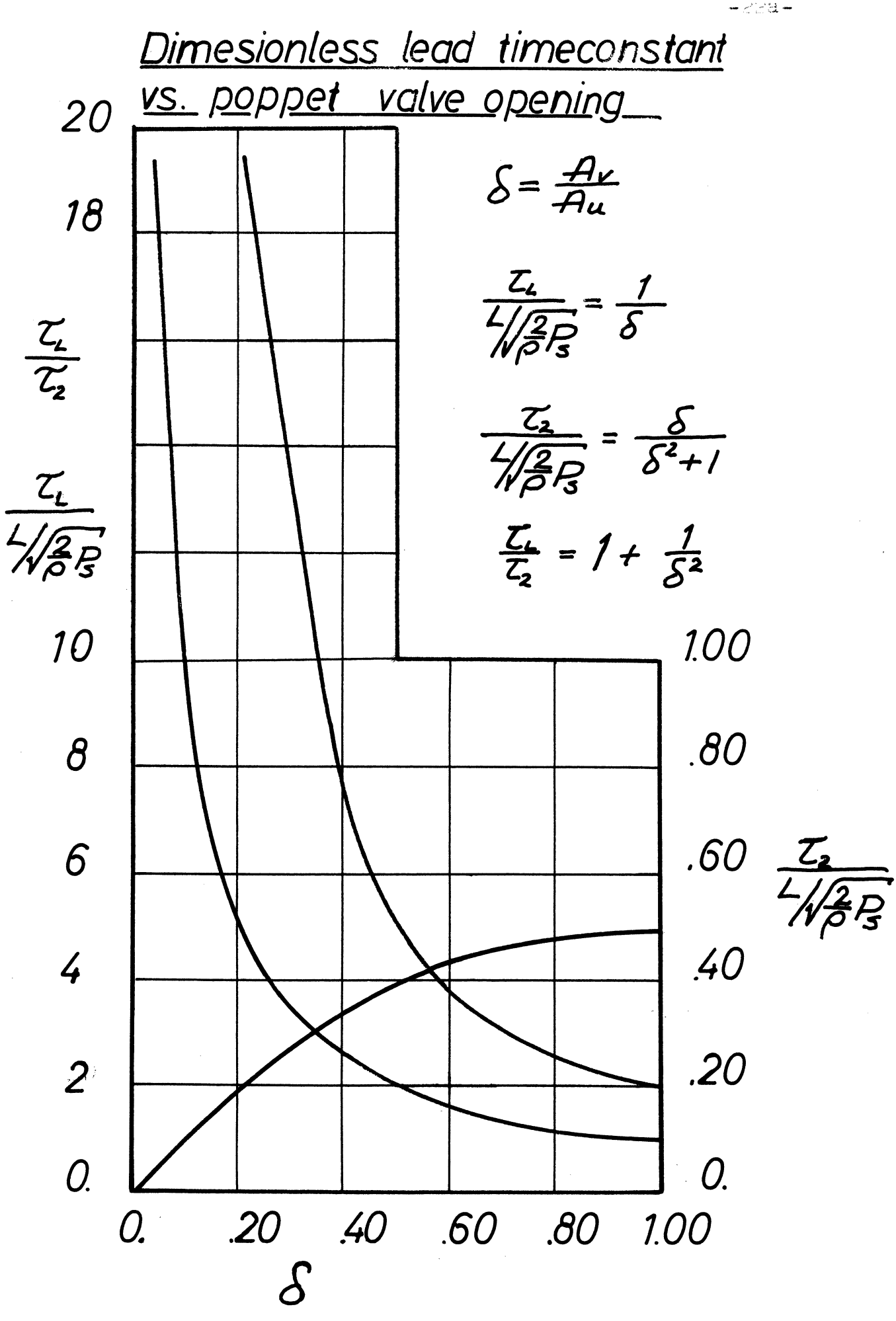
Dimesionless lead timeconstant
vs. poppet valve opening
$\delta = \frac{A_v}{A_u}$
$\frac{\tau_1}{L/\sqrt{\frac{2}{\rho}P_s}} = \frac{1}{\delta}$
$\frac{\tau_2}{L/\sqrt{\frac{2}{\rho}P_s}} = \frac{\delta}{\delta^2+1}$
$\frac{\tau_1}{\tau_2} = 1 + \frac{1}{\delta^2}$
$\frac{\tau_1}{\tau_2}$
$\frac{\tau_1}{L/\sqrt{\frac{2}{\rho}P_s}}$
$\frac{\tau_2}{L/\sqrt{\frac{2}{\rho}P_s}}$
20
18
10
8
6
4
2
0.
1.00
.80
.60
.40
.20
0.
0.
.20
.40
.60
.80
1.00
δ

FIGURE 2-7

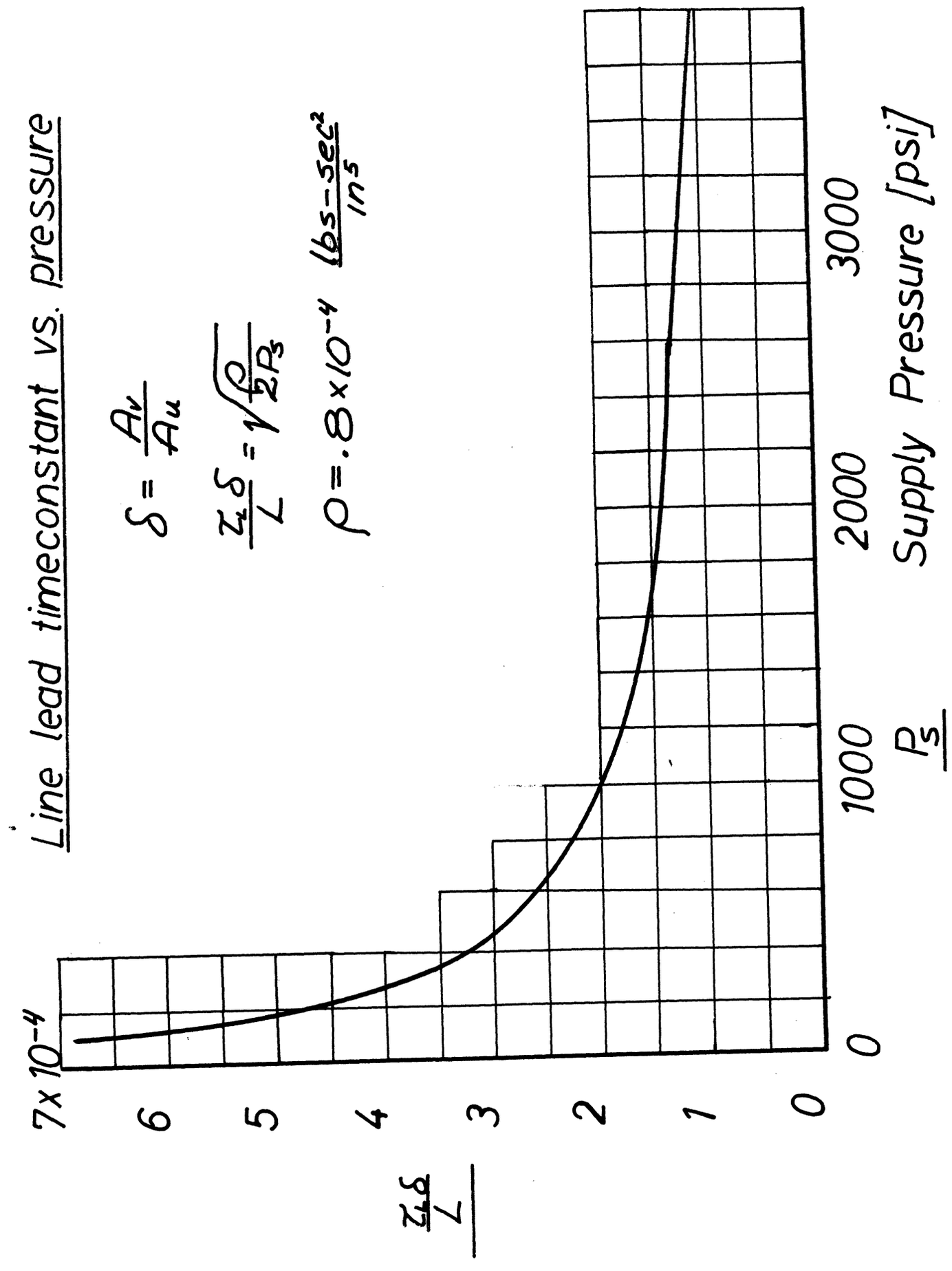
Line lead timeconstant vs. pressure
$\delta = \frac{A_v}{A_u}$
$\frac{4\delta}{L} = \sqrt{\frac{\rho}{2P_s}}$
$\rho = .8 \times 10^{-4}$ lbs-sec²/in⁵
7x 10⁻⁴
6
5
4
3
2
1
0
4δ/L
0
1000
2000
3000
Ps
Supply Pressure [psi]

FIGURE 2-8

From equation (48) we see that this system is always stable as the above inequality always holds. This shows that the inertia force stabilizes the valve, which verifies the physical description given earlier and the component of force due to this lead opposes the valve velocity and acts as positive damping.

2.60 Combined Effects

The previous two sections showed the effect of fluid elasticity and inertia considered separately. These effects can be checked experimentally in a laboratoratory experiment, but in a real model they occur in combination.

In this section the model shown on Figure 2-1a (section 2.1) will be treated in a more general sense. We are still concerned with the lumped parameter model only, and frictionless flow.

Combining the effects of fluid inertia and elasticity give rise to three basic configurations shown in Figure 2-9.

Model a is the straight forward inertia and compressibility effect combined with the poppet valve. Models b and c are two variations of a with the introduction of an upstream resistance. These two models appear alike, but the transfer function (Dynamic characteristics) of

Combined effects models

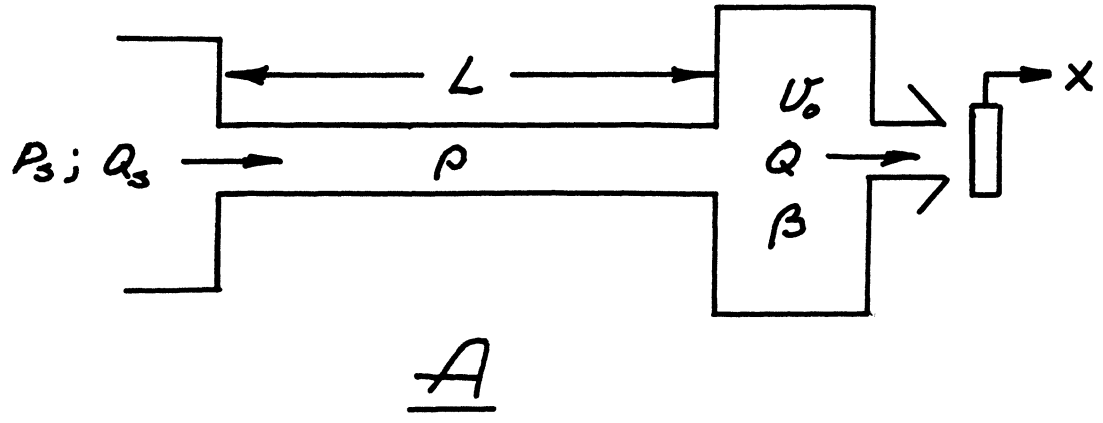

A

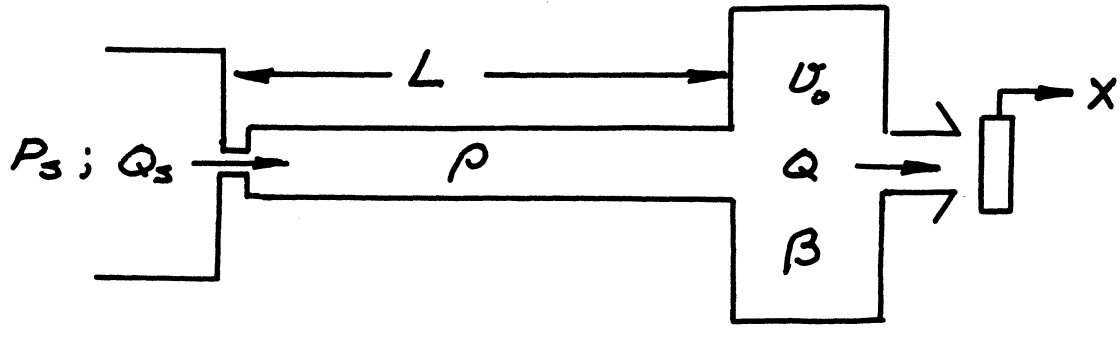

B

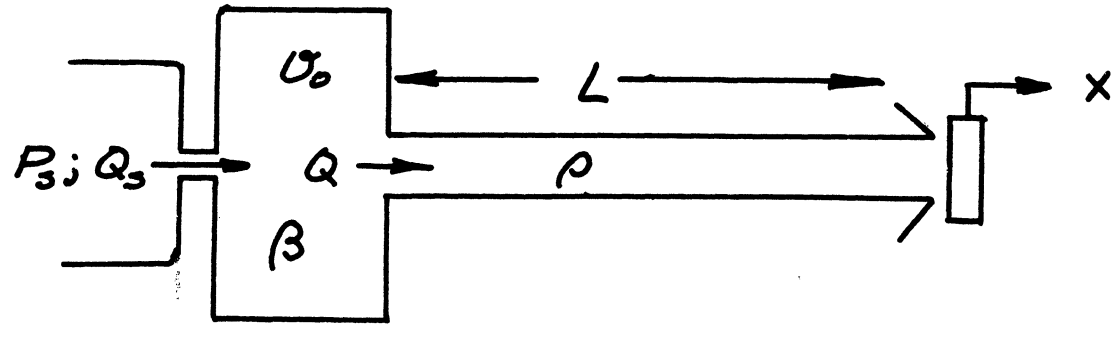

C

FIGURE 2-9

pressure vs. displacement differ. The analysis for these two cases are shown in the Appendix (C-2). Attention will now be focussed on model a.

2.61 Dynamic Equation

The inertia compressibility model under consideration is model a of Figure 2-9. The system consists of a constant pressure source p_s, with a delivery line of length L and crossection A connected to the volume $_o$ and the poppet valve. The downstream condition are steady, p_R assumed constant and arbitrarily set to zero. The fluid has density ρ and elasticity β (psi). In this lumped parameter model all the volume is lumped into $\mathcal{V}_o$ and the line L considered incompressible.

From the previous analysis we expect the system stability to depend on the relative magnitude of the lead (τ_L) and lag (τ_c) time constants from the line and volume models respectively.

System Equations:

Line: $$P = -\left[\frac{\rho L}{A} D + \frac{\rho Q_o}{A^2}\right] Q_s \qquad (53)$$

Volume: $$Q_s - Q = \frac{\mathcal{V}_o}{\beta} DP \qquad (54)$$

Valve: $$Q = K_1 X + K_2 P \qquad (55)$$

$P_R = 0$, K_1 and K_2 are the valve flow coefficients as used previously. By combining and eliminating the flow we get

$$\Delta\left(\frac{P}{X}\right) = -\frac{K\rho Q_0}{\rho Q_0 K_2 + A^2}\left\{\frac{\frac{LA}{Q_0}D+1}{\frac{\left(\frac{U_0}{\beta}\rho LA\right)D^2}{A^2+\rho Q_0 K_2} + \frac{\left(\left(\frac{U_0}{\beta}\right)\rho Q_0 + \rho LAK_2\right)D}{A^2+\rho Q_0 K_2}+1}\right\} \quad (56)$$

which can be written as

$$\Delta\left(\frac{P}{X}\right) = -G_3\,\frac{\tau_L D+1}{A_2 D + A_1 D + 1} \quad (57)$$

where the coefficients are defined by equation (56). By introducing the values for coefficients using $t_L = LA/Q$ and $t_c' = \frac{U}{\beta K_2}$ the equation reduces to

$$G_3 = \frac{2P_3\pi D}{A}\,\frac{\delta}{\delta^2+1} \quad (58)$$

$$A_2 = \tau_L \cdot \tau_c'\,\frac{\delta^2}{\delta^2+1} \quad (59)$$

$$A_1 = (\tau_L + \tau_c')\,\frac{\delta^2}{\delta^2+1} \quad (60)$$

These last equations with equation (57) give the desired functions to look at the combined stability equations.

2.62 Stability

The desired frequency equation is obtained by substituting (57) into (22) and given below

$$\{A_2 MD^4 + A_1 MD^3 + MD^2 + AG_3\tau_L D + G_3 A\}X = 0 \quad (61)$$

Here c and K 0 as a first approximation.

The stability given by B-35 is

$$\left(1-\frac{A_1}{C_L}\right) > \frac{A_2}{A_1}\left(\frac{\tau_L G_3 A}{M}\right) \tag{62}$$

Before substituting we can see two cases here: when the right hand side small or negligible, and when it is large. In order to investigate further we have for the groups involved: in (62)

$$\frac{A_1}{C_L} = \frac{\delta^2}{\delta^2+1}(\sigma+1) \tag{63}$$

$$\frac{A_2}{A_1}\left(\frac{\tau_L G_3 A}{M}\right) = \frac{R}{\delta(\delta^2+1)} \tag{64}$$

$$\sigma \equiv \frac{2 U_0 P_s}{\beta L A} \tag{65}$$

$$R \equiv \left(\frac{2P_s}{\beta}\right)\left(\frac{\rho U_0}{M}\right)\left(\frac{\pi D L}{A(\sigma+1)}\right) \tag{66}$$

Both and R are constants related to the conditions upstream of the poppet. The two conditions now become evident; as $\delta \to 0$ equation (63) becomes zero, but equation (64) tends to infinity. The inequality of (62) is then violated, so at very small displacements the valve should be unstable. Solving (62) gives

$$\delta[\delta^2\sigma+1] > R \tag{67}$$

but for small δ this reduces to

$$\delta > R \tag{68}$$

With $\delta = \frac{\pi D x_o}{A}$ this becomes

$$x_o \geq \left(\frac{2P_s}{\beta}\right)\left(\frac{\rho U_o}{M}\right)\left(\frac{L}{\sigma+1}\right) \tag{69}$$

Equation (69) gives the stability limit for small valve displacements. For stable operation x_o must be greater than the right hand side of (69).

The other two roots to this equation can be found by using equation (67) for the condition $R \rightarrow 0$ and δ large. This yields

$$\delta \leq \pm\sqrt{\frac{\beta L A}{2U_o P_s}} \tag{70}$$

or

$$x_o \leq \pm\frac{D}{4}\sqrt{\frac{\beta}{2P_s}\frac{LA}{U_o}} \tag{71}$$

Equation (71) only makes sense for values of the square root less then unity as x_o larger than D/4 does not represent a solution (or $\delta > 1$, either). Combining

(67) and (71) we have.

$$\left(\frac{2P_3}{\beta}\right)\left(\frac{\rho U_o}{M}\right)\left(\frac{L}{\sigma+1}\right) \leq X_o \leq \frac{D}{4}\sqrt{\frac{\beta}{2P_3}\frac{LA}{U_o}} \qquad (72)$$

Equation (72) then describes the desired stability limit on displacement of the poppet valve. If the external spring is included the stability equation becomes:

$$\delta\left\{(1+S)+\delta^2\left[1-(\sigma+1)\frac{\eta(\sigma+1)+1}{\eta\delta^2(\sigma+1)+1}\right]\right\} > R\left\{1+\eta\delta(\sigma+1)\right\} \qquad (73)$$

$$S = \frac{K}{M}\frac{\rho U_o L}{\beta A} \qquad (74)$$

$$\eta = \frac{K}{2P_3\pi D} \qquad (75)$$

For δ small, this becomes

$$\delta > \frac{R}{(1+S)-R\eta(\sigma+1)} \qquad (76)$$

Figure 2-10 shows the general trend of equation (76) as a function of η , the nondimensional spring rate. Figure 2-10 shows δ tends to infinity at $\eta^{*\prime}$ when the denommator of (76) vanishes, but of more interest would be when δ approaches unity, given by η^*

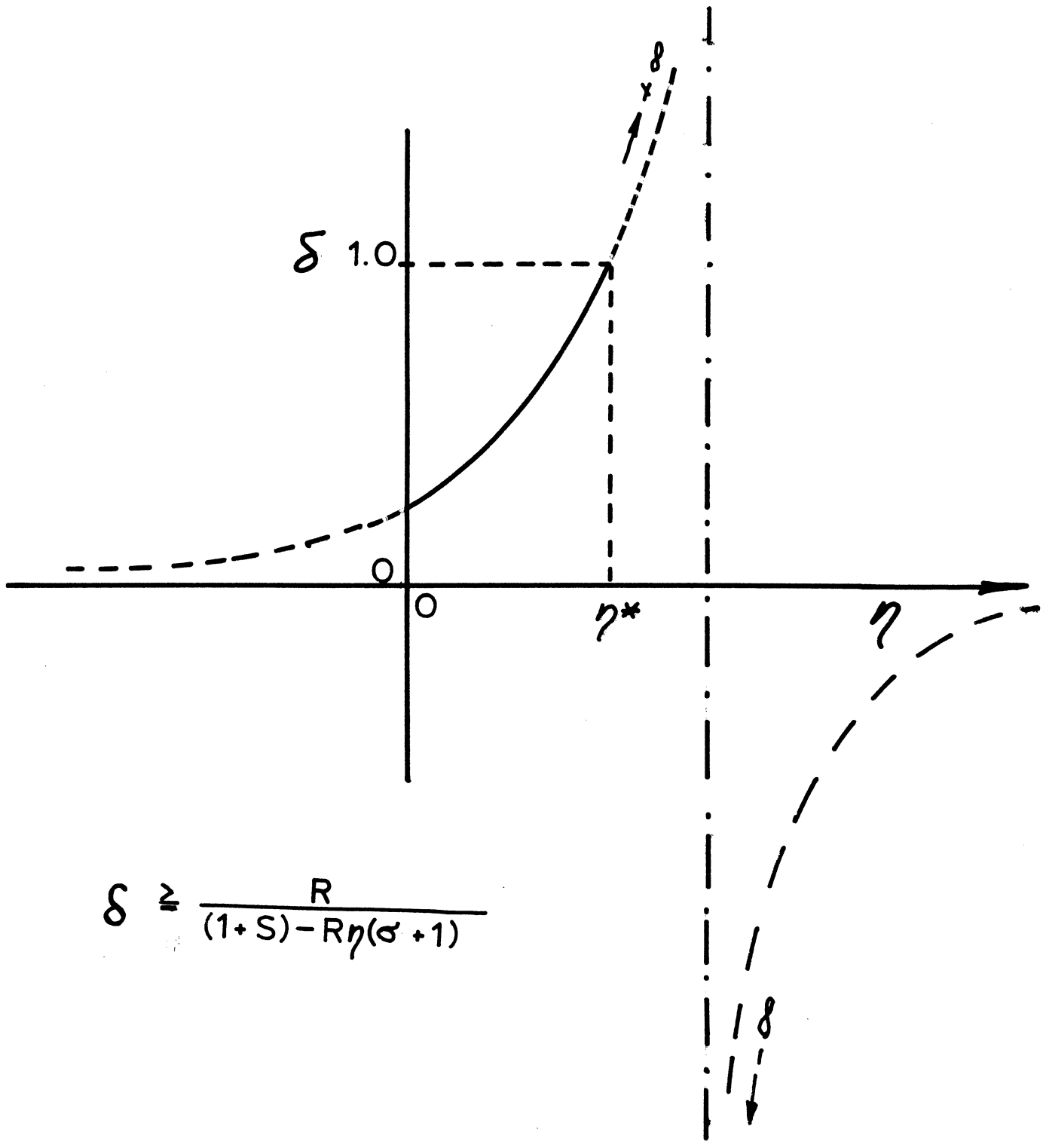

$$\delta \geq \frac{R}{(1+S) - R\eta(\sigma+1)}$$

FIGURE 2-10

$$\eta^x = \frac{R-(1+S)}{R(S+1)} \qquad (78)$$

If then $\eta \leq \eta^x$ a point of stable operation exists.

2.70 Downstream Effect

Downstream effects are connected with the possibility of pressure variations behind the poppet due to fluid motion.

These are due to both fluid inertia and compressibility, but also are strongly affected by the fluid vorticity and turbulant mixing from the jet as it leaves the poppet.

Previous investigators (Stone Ref#2) noted that a poppet stable when exhausting into a "infinite" downstream chamber would oscillate when confined by a circular tube, indicating that the change in flow pattern caused by downstream effects and largly due to fluid compressibility. A simplified analysis will show the adverse effect that this may cause.

2.71 Downstream Compressibility

A simplified system is shown in Figure 2-11a where it is assumed the upstream pressure p_s is constant, the downstream volume is $_R$ and the restriction is given by A_R. By similarity we know that the equations are those of section 2.40 so we can write down the result as:

$$\Delta\left(\frac{P_L}{X}\right) = \frac{G_R}{\tau_R D + 1} \tag{79}$$

where

$$G_R = \frac{K_1}{K_4 + K_5} \tag{80}$$

$$\tau_R = \frac{V_R}{\beta(K_4 + K_5)} \tag{81}$$

K_4 and K_5 are the flow coefficients with respect to pressure for valve and downstream restriction. The dynamic equation in this case depends on the downstream construction of the poppet as shown on Figure 2-11 b. In this case we have

$$P_s A + P_R A_a - F_o - C\dot{X} - KX = M\ddot{X}$$

which for linearized considerations yield, with equation (79) substituted for p_a:

$$\left\{M\tau_R D^3 + (M + \tau_R C)D^2 + (C + \tau_R K)D + (K - G_R A_a)\right\} = 0 \tag{82}$$

For stability: (Ref. Appendix C)

$$a_1 a_2 > a_3 a_0 \tag{83}$$

$$a_0 > 0 \tag{84}$$

Equation (84) then gives

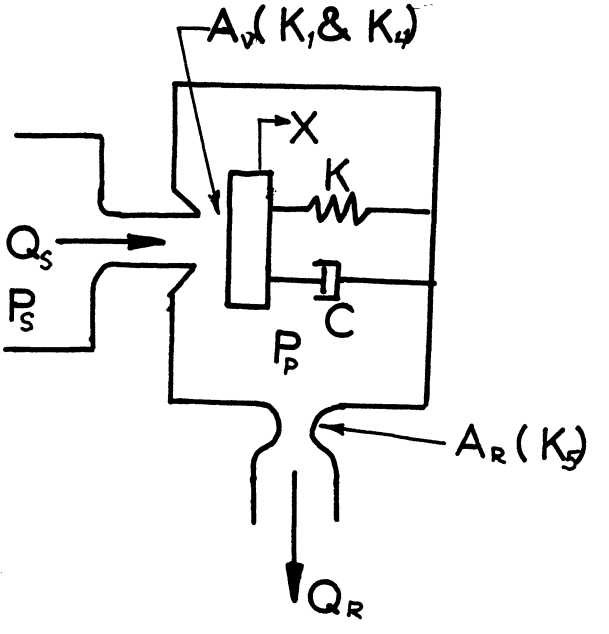

(A) SCHEMATIC

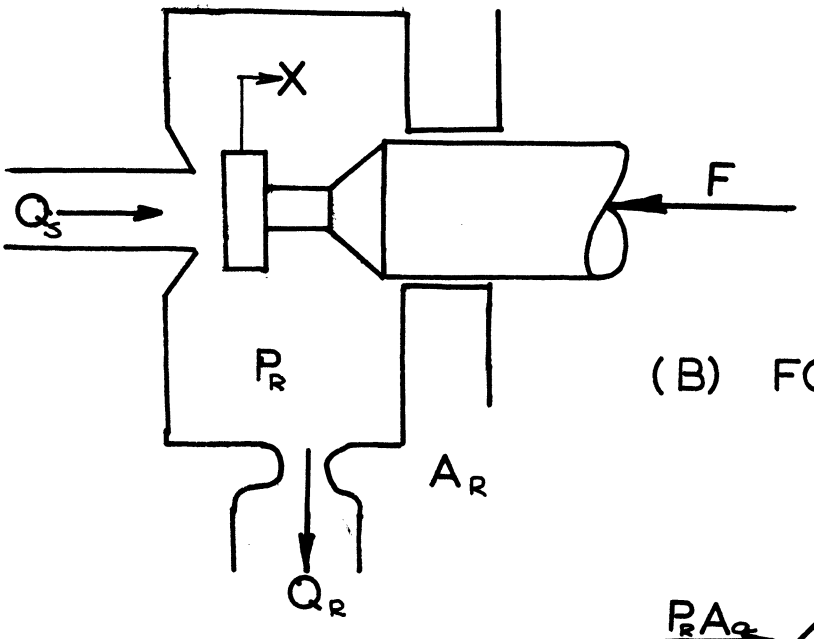

(B) FORCES

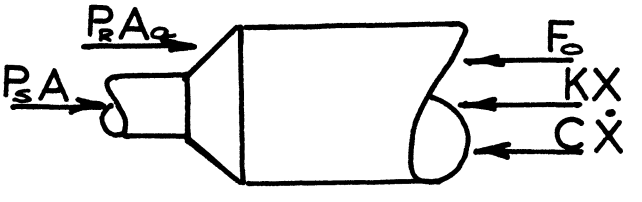

DOWNSTREAM COMPRESSIBILITY

FIGURE 2-11

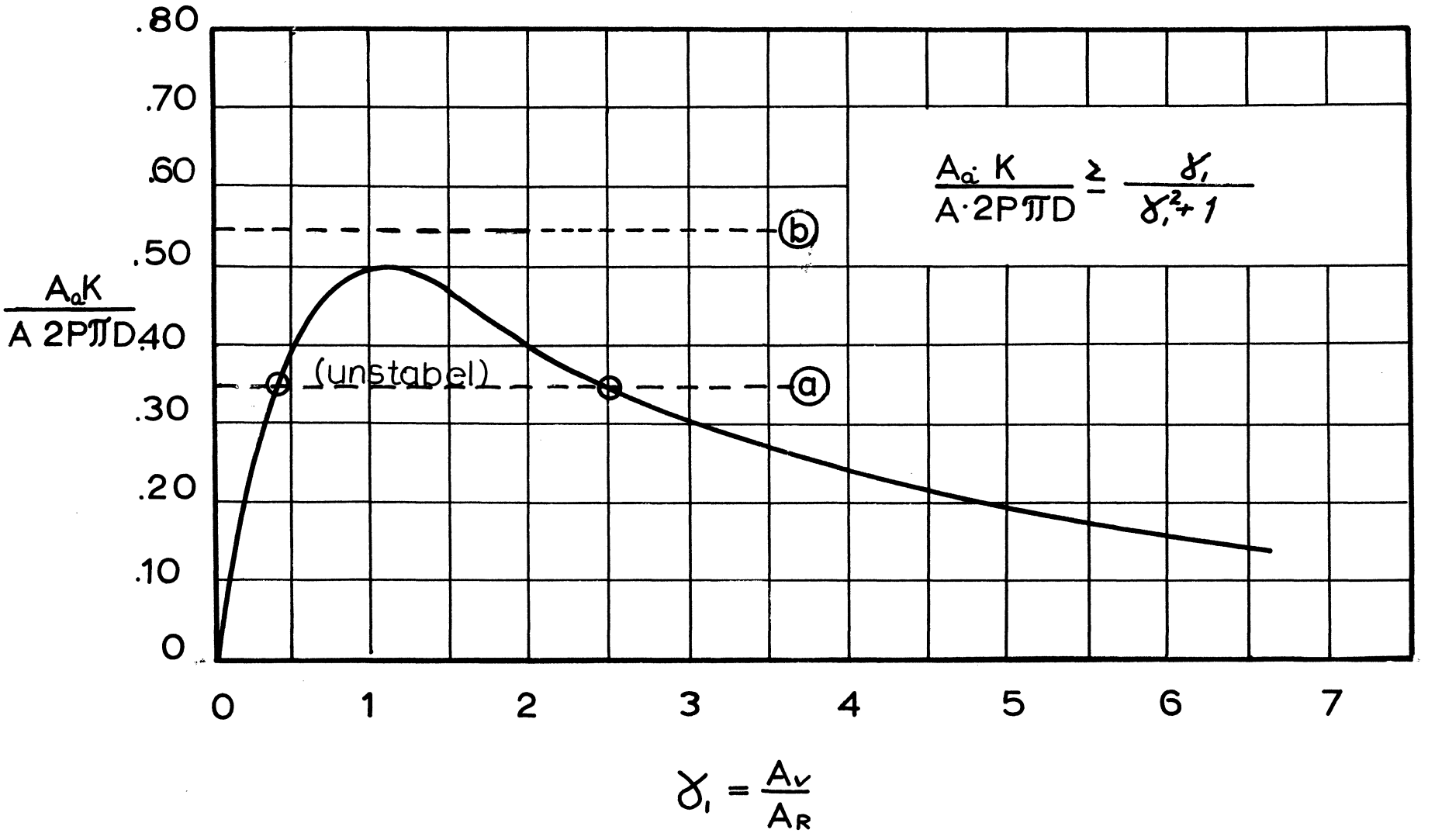

COMPRESSIBILITY, GAIN VS VALVE POSITION

$$K \geq G_R A_a \tag{85}$$

or when substituted for G_R:

$$\frac{A_a}{A} \frac{K}{2P_s \pi D} \geq \frac{\gamma_1}{\gamma_1^2+1} \tag{86}$$

where

$$\gamma_1 = \frac{A_v}{A_R} \tag{87}$$

Figure 2-12 shows the behavior of equation 86, and for the two values of K in a and b. The value of b is always stable, while a has the unstable region given by the intersection of the line with the curve defined by Equation 8b.

Part III Experimental Results

3.00 Background

The experimental apparatus and test procedure is briefly outlined in Appendix A-1. The experimental results are divided into three groups, Static Characteristics, Dynamic Forces, and Stability. In Appendix D are shown the flow coefficients for the fixed orifices and the poppet valve. These values are used in evaluating the results.

All the results presented are for a flat poppet of diameter d = .750 inches and the diameter of upstream

line and the nozzle is D = .125 inches.

3.10 Static Characteristics

The static force and pressure curves are shown in Figures 3-1 and 3-2. Figure 3-1 represents the force for constant upstream pressure. Figure 3-2 shows the force and upstream pressure when fixed orifice A_u is introduced. The dashed curves represent the theory given by equation (12 and Figures 2-3 with the response to a large input, slowly varying, sine wave. The output is seen to be nonlinear as expected with the peak pressures less than the theory predicts. The discrepancies are largly due to the variations in flow coefficients, especially that of the poppet valve. (Ref. Fig. D-2).

Again Figure 3-2 gives indications on the (low frequency) output to be expected as function of valve mean position.

3.20 Dynamic Characteristics

In this section the validity of the equations developed in sections 2-40 and 2.50 were checked out. The poppet valve is excited sinusoidally and the force, displacement and upstream pressure is recorded and compared to the theory.

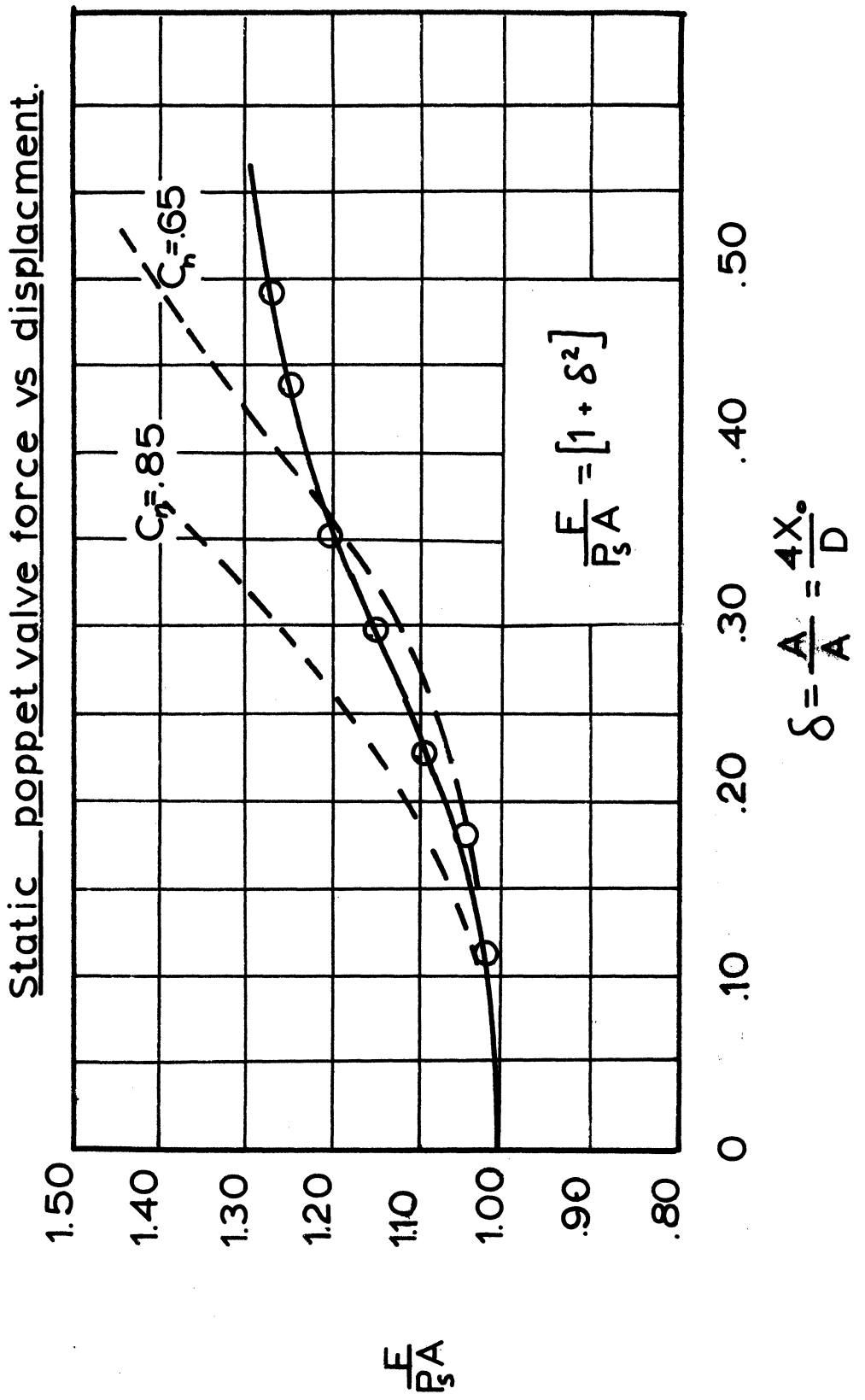
Static poppet valve force vs displacment.
C_n=.85
C_n=.65
$\frac{F}{P_s A} = [1 + \delta^2]$
$\delta = \frac{A}{A} = \frac{4X_o}{D}$
$\frac{F}{P_s A}$
1.50
1.40
1.30
1.20
1.10
1.00
.90
.80
0
.10
.20
.30
.40
.50

FIGURE 3-1

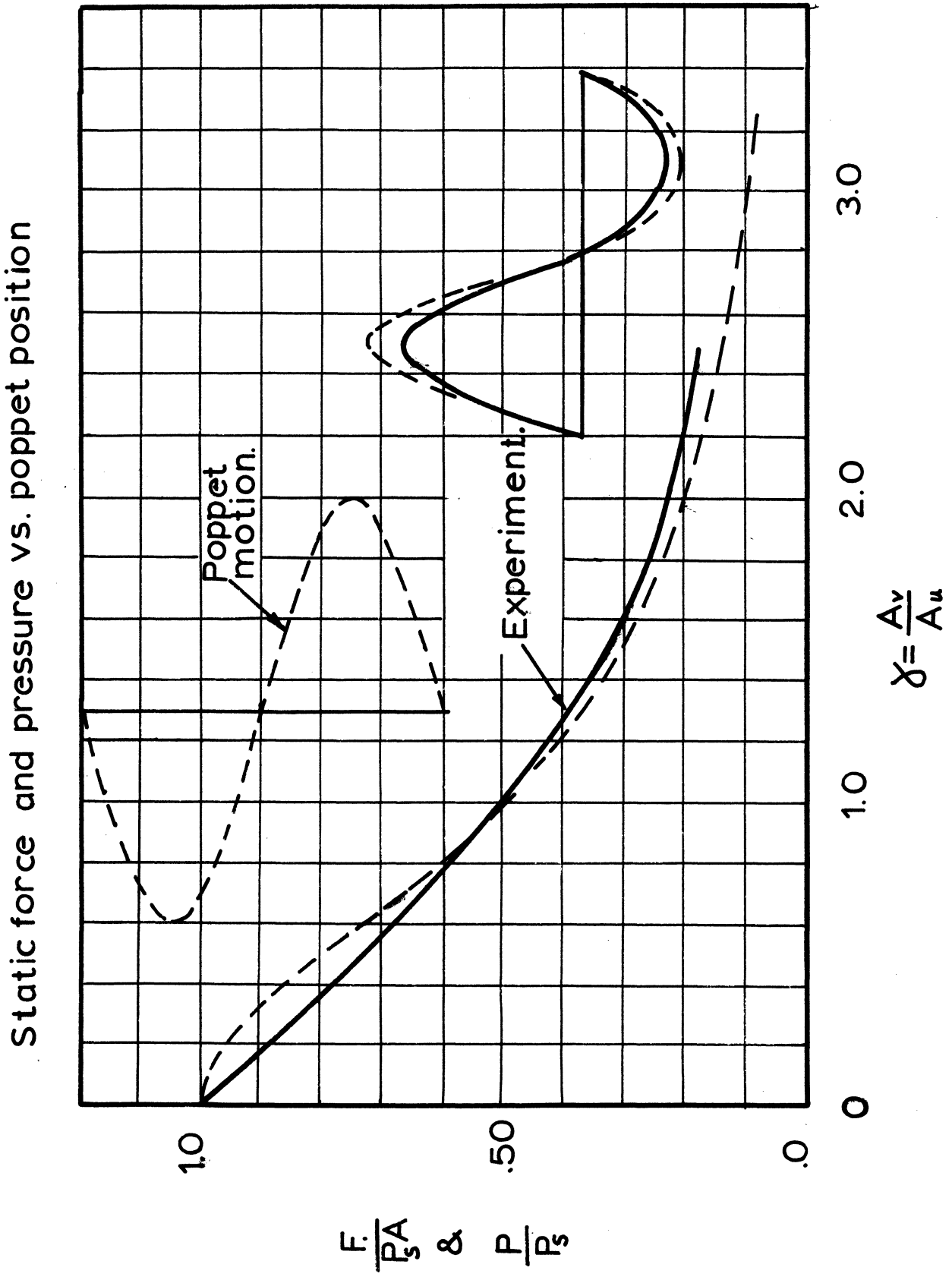
Static force and pressure vs. poppet position
Poppet motion.
Experiment.
1.0
.50
0.
0
1.0
2.0
3.0
$\gamma = \frac{A_v}{A_u}$
$F \cdot \frac{1}{P_s A}$ & $\frac{P}{P_s}$

FIGURE 3-2

Since the apparatus is frequency limited (operating range only from 0-45 cps) the magnitude of the upstream geometry was magnified to create measurable lead and lag values for pressure and force.

The results from this part are shown in Figures 3-3 through 3-7.

3.21 Compressibility

A. Results:

The system tested is that shown on Figure 2-1b. In the experimental set-up both $\mathcal{V}_o$ and A_u are changable as well as the mean valve position γ_o (or x_o). Figure 3-3 shows the phase lag ϕ between either force or pressure with displacement as a function of system volume. Figure 3-4 shows the effect of changing both volume and valve mean operating postion. Figure 3-5 shows a crossplot of data obtained from Figures 3-3 and 3-4 on a nondimensional basis and is to be compared with the value of equation (37).

B. Discussion

The results of Figure 3-5 follow the theory well. The value used for β is 250,000 psi, which is high when it is considered that the oil has air entrained that will reduce this value. The peculiarity

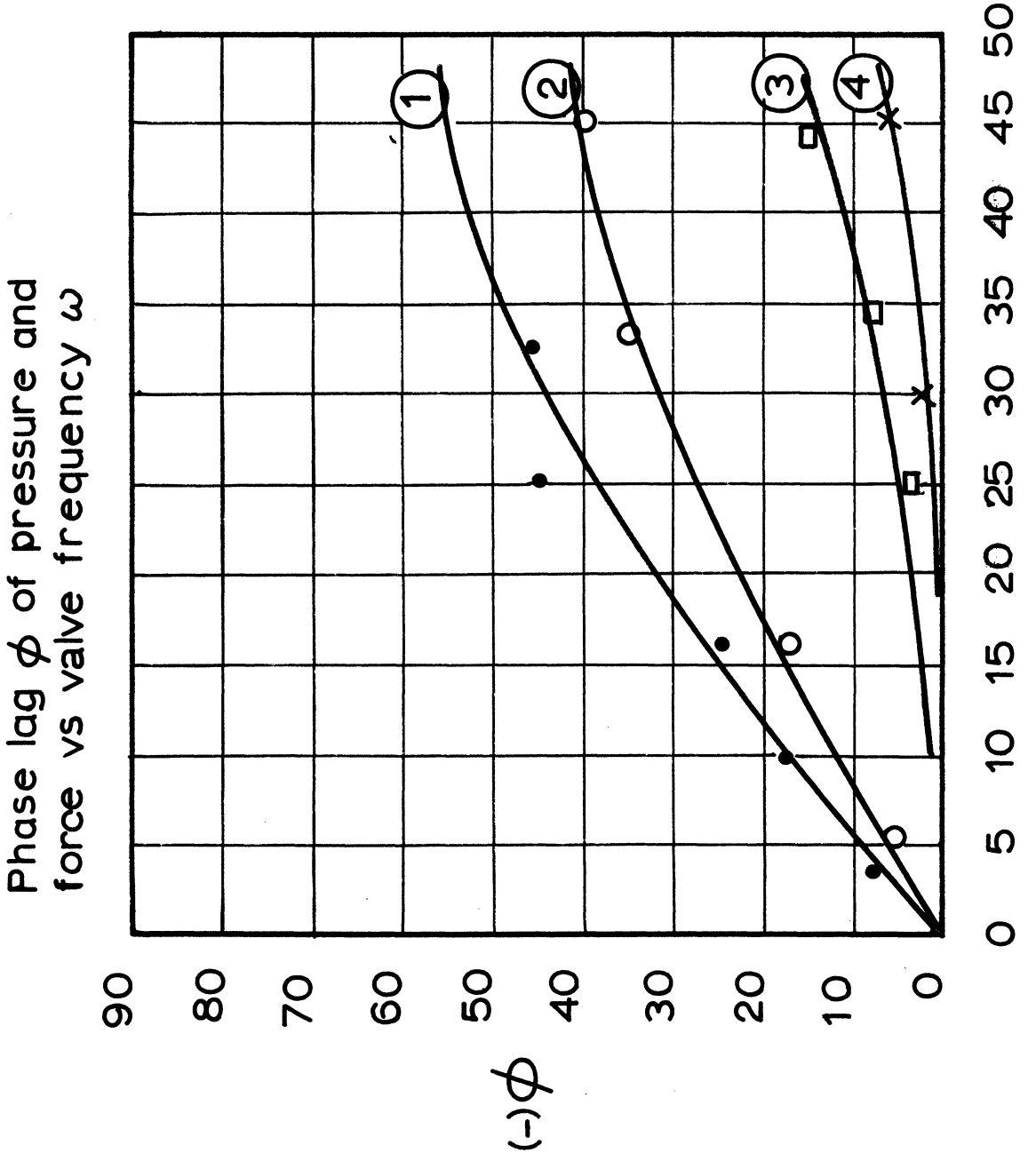
Phase lag ϕ of pressure and force vs valve frequency ω
γ & P_s constant.
1 — v_o = 10 cu.in.
2 — v_o = 5 cu. in.
3 — v_o = .50 cu. in.
4 — v_o = .05 cu. in.
(-)ϕ
0 10 20 30 40 50 60 70 80 90
0 5 10 15 20 25 30 35 40 45 50
ω CPS.
1
2
3
4

FIGURE 3-3

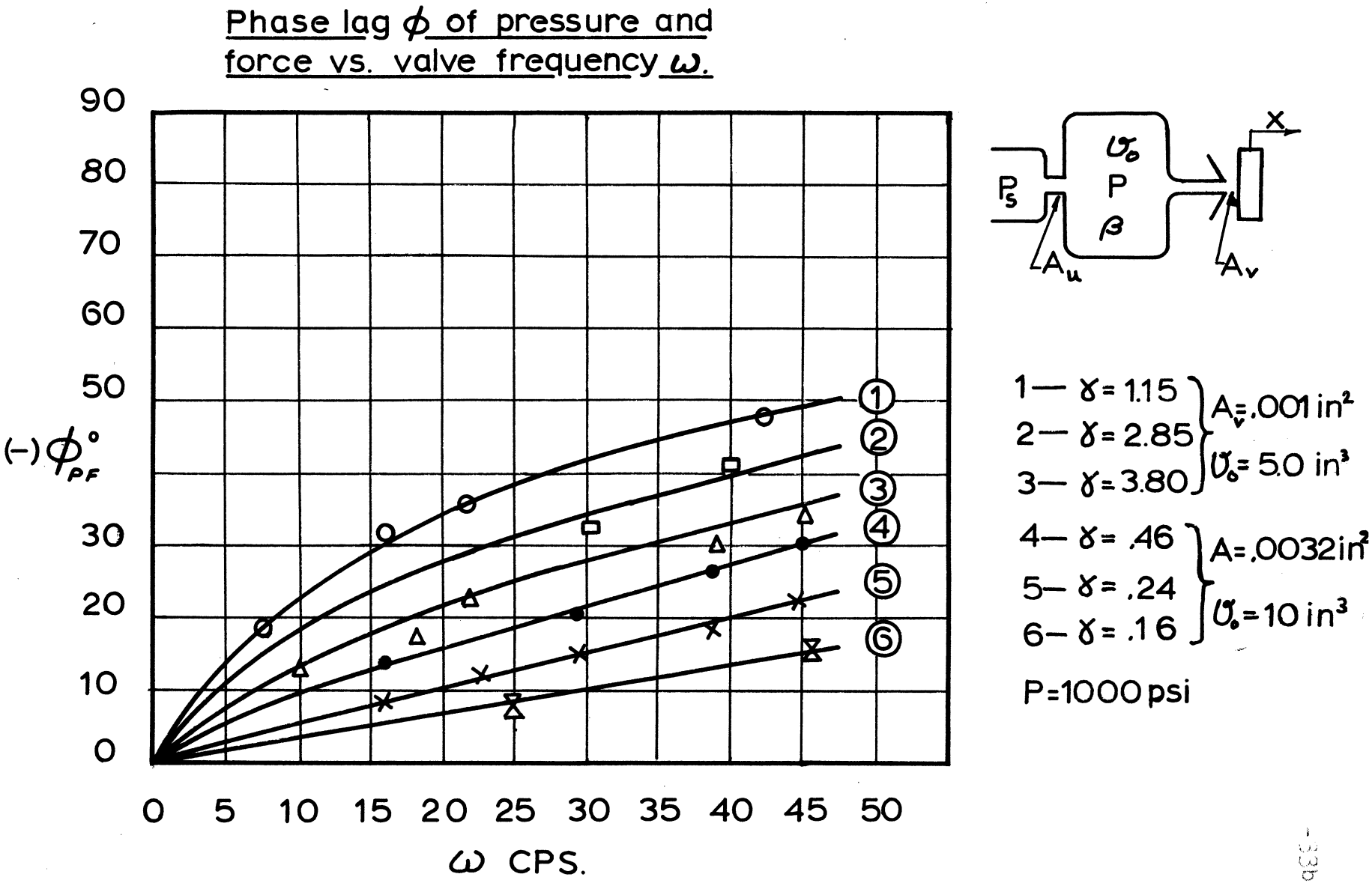
Phase lag ϕ of pressure and force vs. valve frequency ω.
90
80
70
60
50
30
20
10
0
$(-)\phi_{PF}^{\circ}$
0 5 10 15 20 25 30 35 40 45 50
ω CPS.
V_o
P
β
P_s
A_u
A_v
X
1— γ = 1.15
2— γ = 2.85
3— γ = 3.80
A_v = .001 in²
V_o = 5.0 in³
4— γ = .46
5— γ = .24
6— γ = .16
A = .0032 in²
V_o = 10 in³
P = 1000 psi

FIGURE 3-4

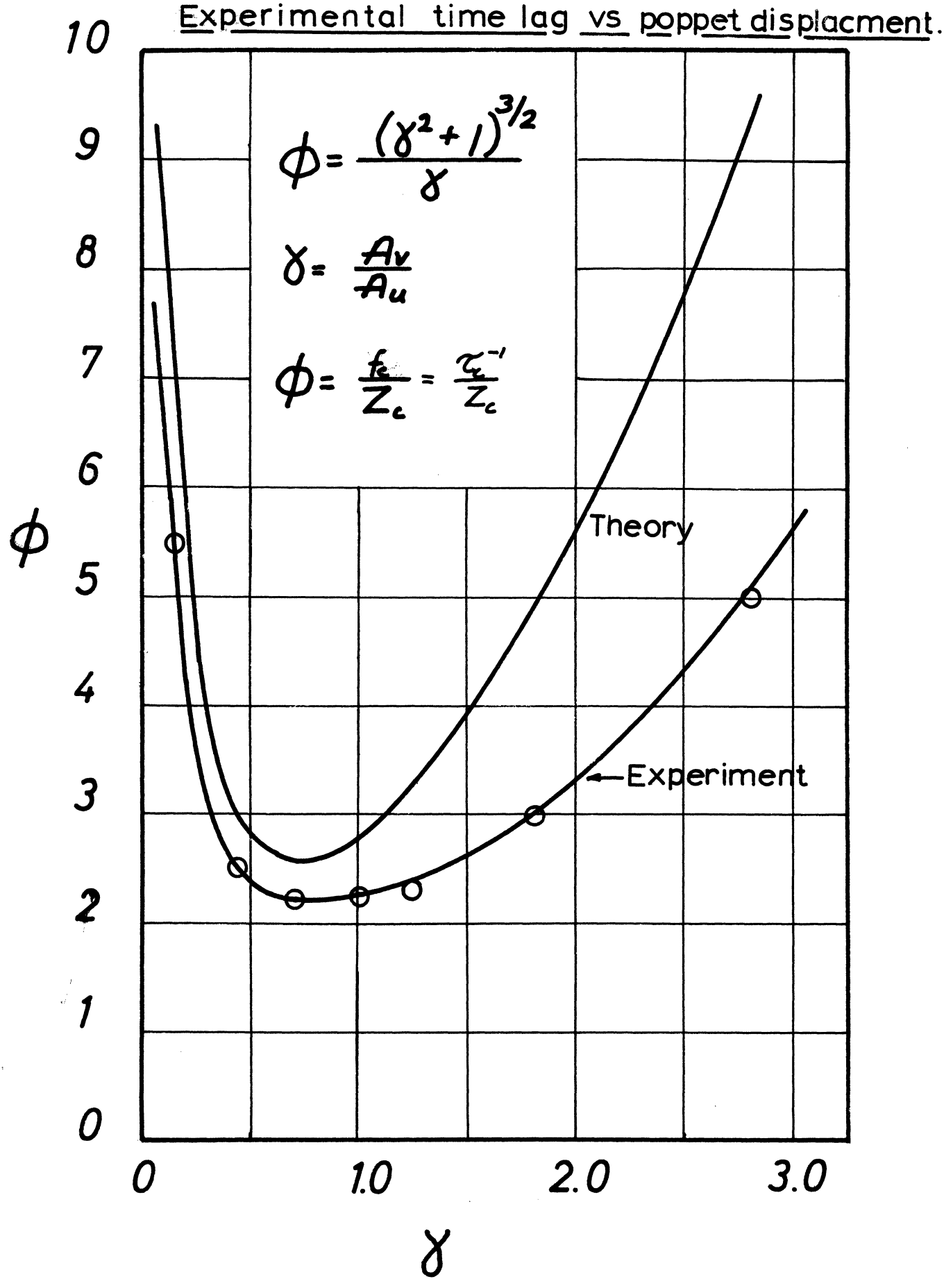
Experimental time lag vs poppet displacment.
$\phi = \frac{(\gamma^2+1)^{3/2}}{\gamma}$
$\gamma = \frac{A_v}{A_u}$
$\phi = \frac{f_c}{Z_c} = \frac{\tau_c^{-1}}{Z_c}$
Theory
Experiment
ϕ
γ
0
1
2
3
4
5
6
7
8
9
10
0
1.0
2.0
3.0

FIGURE 3-5

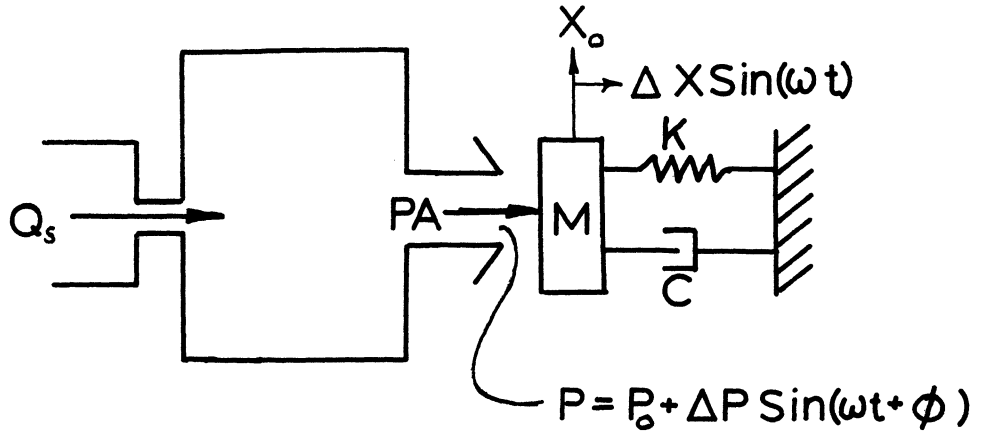

$$\Delta\left(\frac{P}{X}\right) = -G_1 \frac{1}{\tau_c D + 1} = -G_1(j\omega)$$

Newtons law.

$$(\Delta P)A - C\dot{X} - KX = M\ddot{X} \quad \text{or:}$$

$$\underline{-G_1(j\omega)A - KX - C\dot{X} - M\ddot{X} = 0}$$

VECTOR DIAGRAM

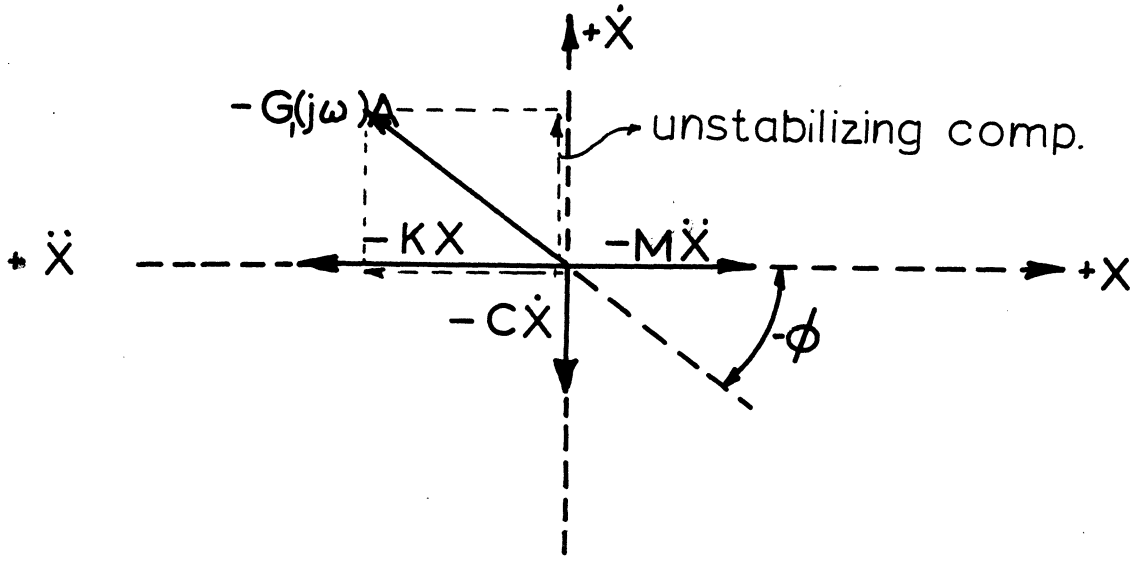

LAG EFFECTS

FIGURE 3-6

of this curve is obvious from equation (34) where t_c is seen inversely proportional to the sum of the flow coefficients with pressure. It can be seen that K_3 starts at infinity for small and decreases, while K_2 starts at zero and increase. The sum then gives for the resultant equation a maximum for t_c (or minimum for f_c) at $\gamma = .707$. The experimental value here agreed well.

Since the excitation frequency of the poppet is low, the inertia force due to the poppet motion is negligible and the fluid forces were measured directly by the force gage. The result was, then, that the fluid forces were those caused by the fluid pressure and in phase with the pressure. For the case of compressibility this is a simple lag. Figure 3-6 shows a summary of the results and the force diagram shows the resultant pressure force and that it has a component in the direction of the velocity so that it is unstabilizing.

3.22 Inertia Effects

A. Results

The inertia model tested was that given by Figure 2-5 in the analysis, and the results are presented in Figures 3-7 and 3-8. Figure 3-7 shows guantitatively the variation of the phase lead of pressure and force against

valve displacement and pressure. Figure 3-8 contains all the data obtained for variation of the parameter, cross plotted on a nondimensional form.

B. Discussion

The agreement between the theory and model was initially off by 20% at the most, but by including frictional losses and entrance loss due to the constriction at both the valve and source and, the theory and experiments agree well.

The experiment shows that the inertia force gives rise to a phase lead and that this is realized resist in short lines. Figure 2-9 shows a summary of the system with the transfer function $G(j\omega)$ substituted into the dynamical equation and this shows that the inertia force has a component proportional to the velocity, but opposing it and thereby acts as positive damping, hence stabilizing the valve.

The effect of friction can be lumped and considered as a restriction (Ref. Appendix C-1) and reduces the time lag predicted.

3.30 Stability

Stabilizing the poppet was done by applying a constant force $F_o = p_B A_B$ and having the poppet suspended by a

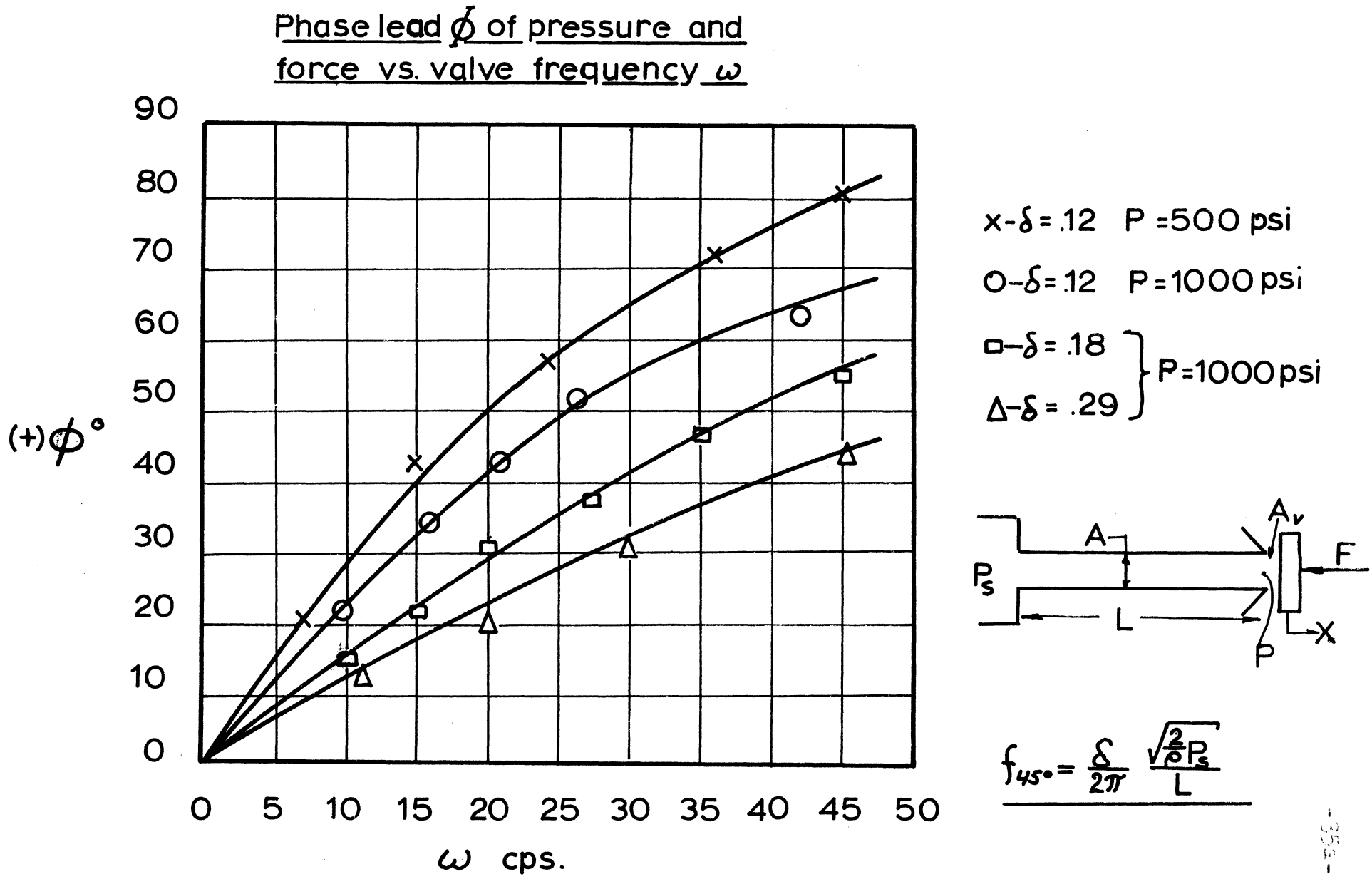
Phase lead ϕ of pressure and force vs. valve frequency ω
(+)ϕ°
90
80
70
60
50
40
30
20
10
0
0 5 10 15 20 25 30 35 40 45 50
ω cps.
x-δ = .12 P = 500 psi
O-δ = .12 P = 1000 psi
□-δ = .18
Δ-δ = .29
P = 1000 psi
A_v
A
F
P_s
L
X
P
$f_{45°} = \frac{\delta}{2\pi} \frac{\sqrt{\frac{2}{\rho} P_s}}{L}$

FIGURE 3-7

Line lead time constant vs. poppet valve position

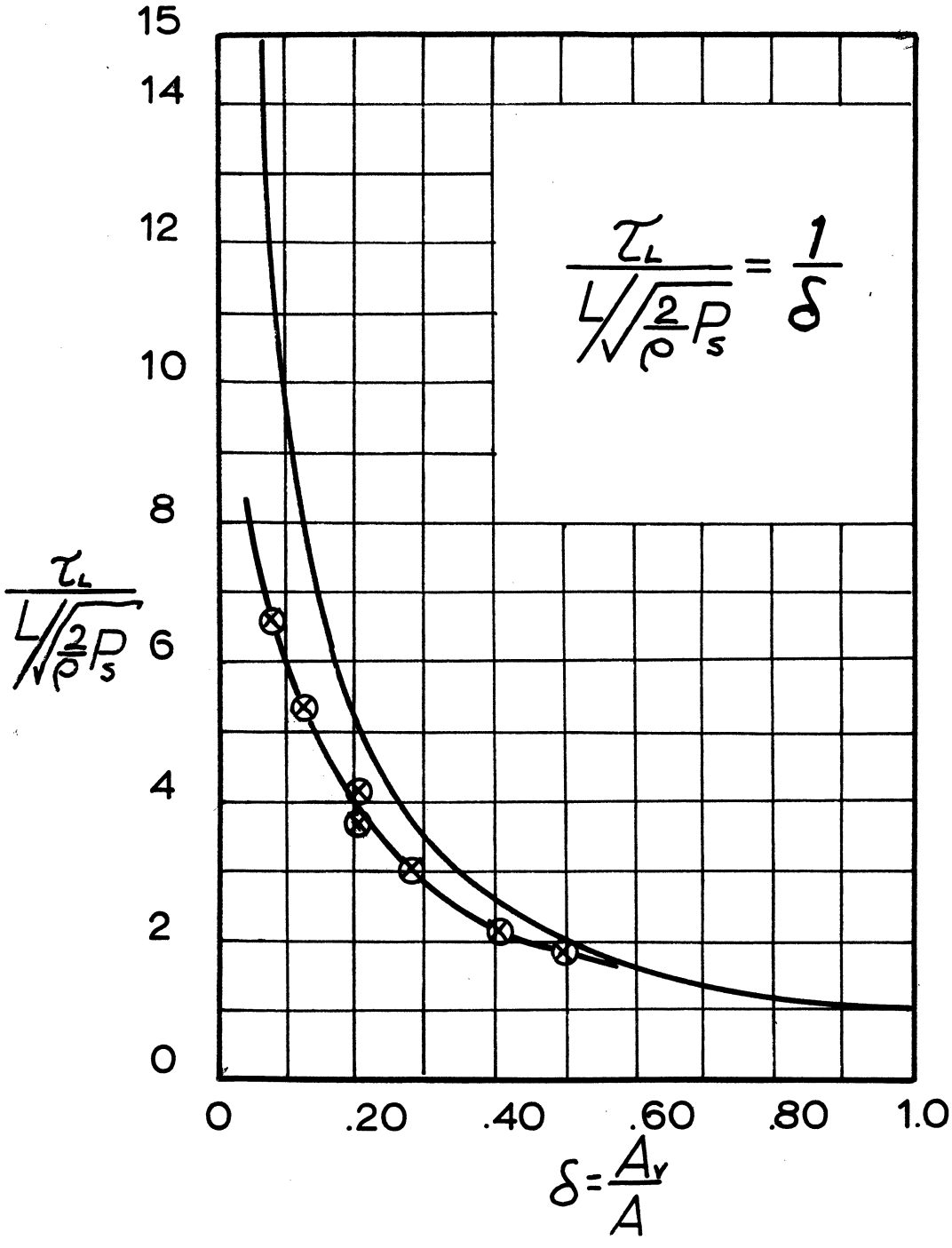

FIGURE 3-8

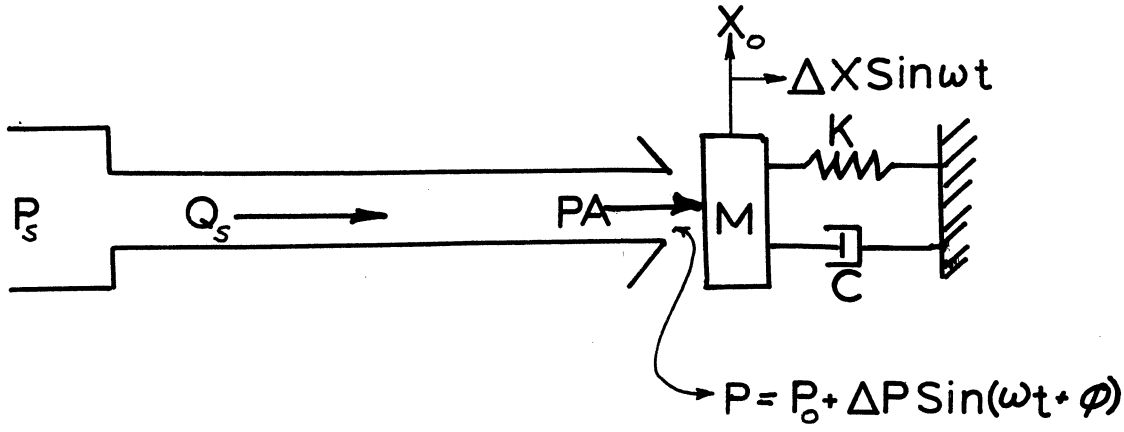

$$\Delta\left(\frac{P}{X}\right) = -G_2\frac{\tau_1 D + 1}{\tau_2 D + 1} = -G_2(j\omega)$$

Newton.

$$(\Delta P)A - C\dot{X} - KX = M\ddot{X} \quad \text{or}$$

$$\underline{-G_2(j\omega)A - KX - C\dot{X} - M\ddot{X} = 0}$$

VECTOR DIAGRAM.

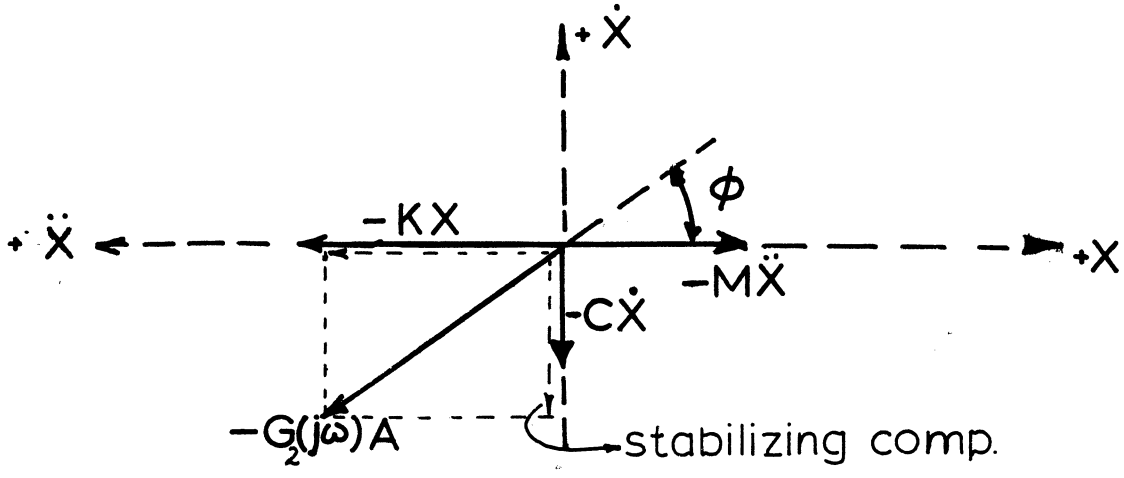

LEAD EFFECTS

FIGURE 3-9

cantilevered spring. The system damping is practically zero when there is no hydraulic pressure applied.

The mean position of the poppet was stepwise changed and at each position it was plucked. If the ensuing vibration died out, it was considered stable. This method, even though crude, has a fair degree of accuracy.

3.31 Simplified Models

A. Compressible Model This model was always found unstable as expected. The frequency of oscillation was given by the combination of the hydraulic and applied spring rates and the poppet mass.

B. Inertia Model This was found stable, but for small displacement, it was unstable. The reason here is that at small displacements, the volume interaction of the line becomes important and the system approaches that of the combined effects reported next.

3.32 Combined Effects

The stability of what may be considered a more realistic system was tested here. The system is that analysed in section 2.60, and shown on Figure 2-9a. In

these tests the line length L, volume $\mathcal{V}_o$ and the supply pressure p_s were varied against the valve displacement. The results are shown in Figures 3-10 through 12. Again Figure 3-12 represents a cross plot of Figures 3-10 and 11.

The results are here compared again to the theory for equations (68) and (69). The experiment only checked the stability for the lower limit, i.e. $\delta \to 0$. The upper limit had no meaning here as the square root in equation (70) was always larger than unity. The system was then stable for values larger than the experimental curves.

Within experimental error the experiment agreed well with the theory, and it showed that the equations definitely had validity. Two main factors contributed to the difference in the experimental results with the theory; the value for β of 250,000 psi is too high and frictional effects decrease the effect of the lead and raise the stability limit, as indicated by the previous experiments.

3.30 Downstream Effects

A qualified analysis of this was not made, but during the experimental investigation oscillations

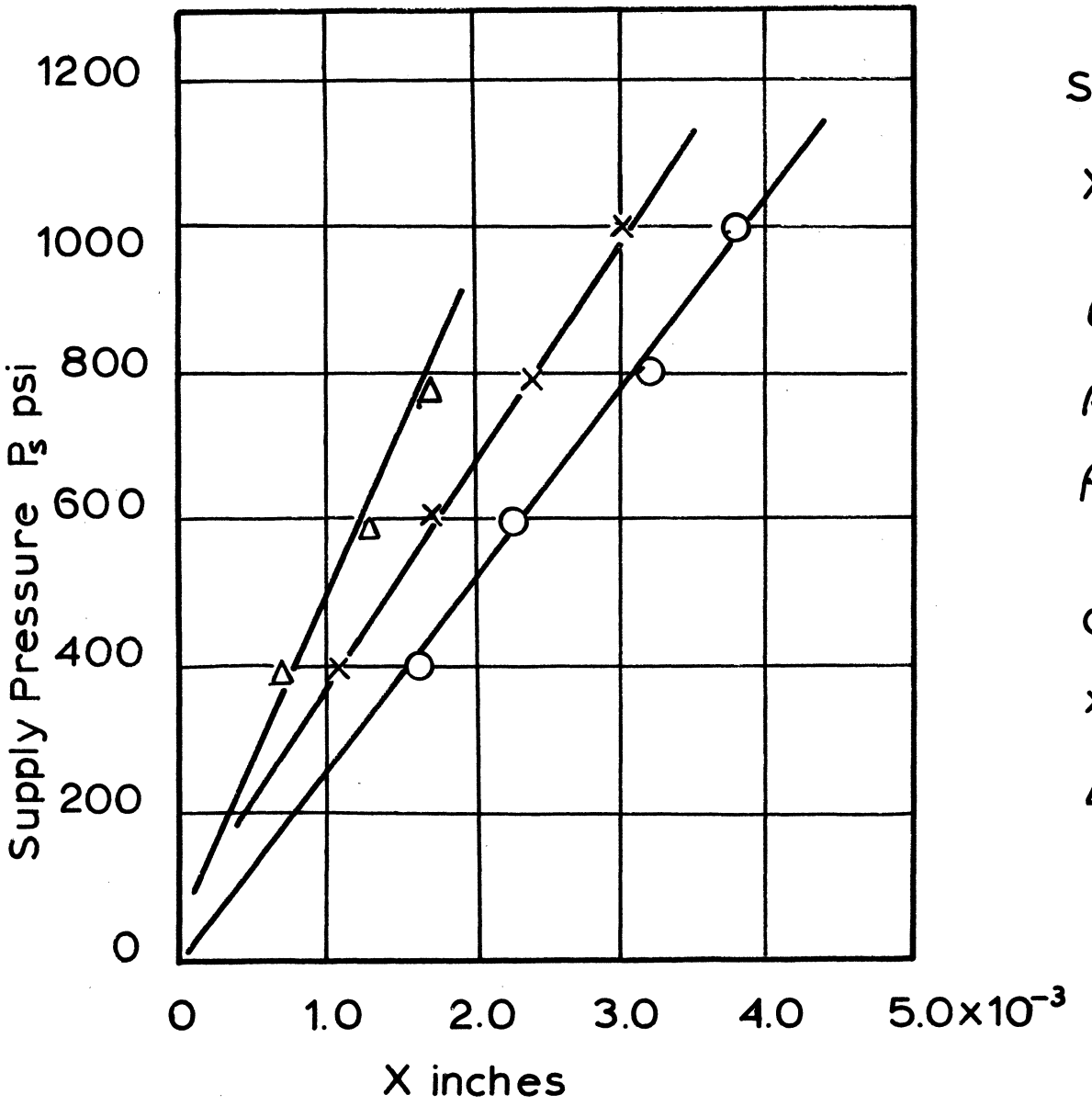

System stable for :

$$X \geq \left[\frac{2\rho V_o}{M\beta}\right] L \times P$$

V_o = 1.00 cu. in.

β = 250 000 psi

$\rho = .80 \times 10^{-4}$ lbs-sec/in^5

O – L = 12 inches

x – L = 8 inches

Δ – L = 4 inches

FIGURE 3-10

SYSTEMS STABILITY VS PRESSURE AND DISPLACMENT.

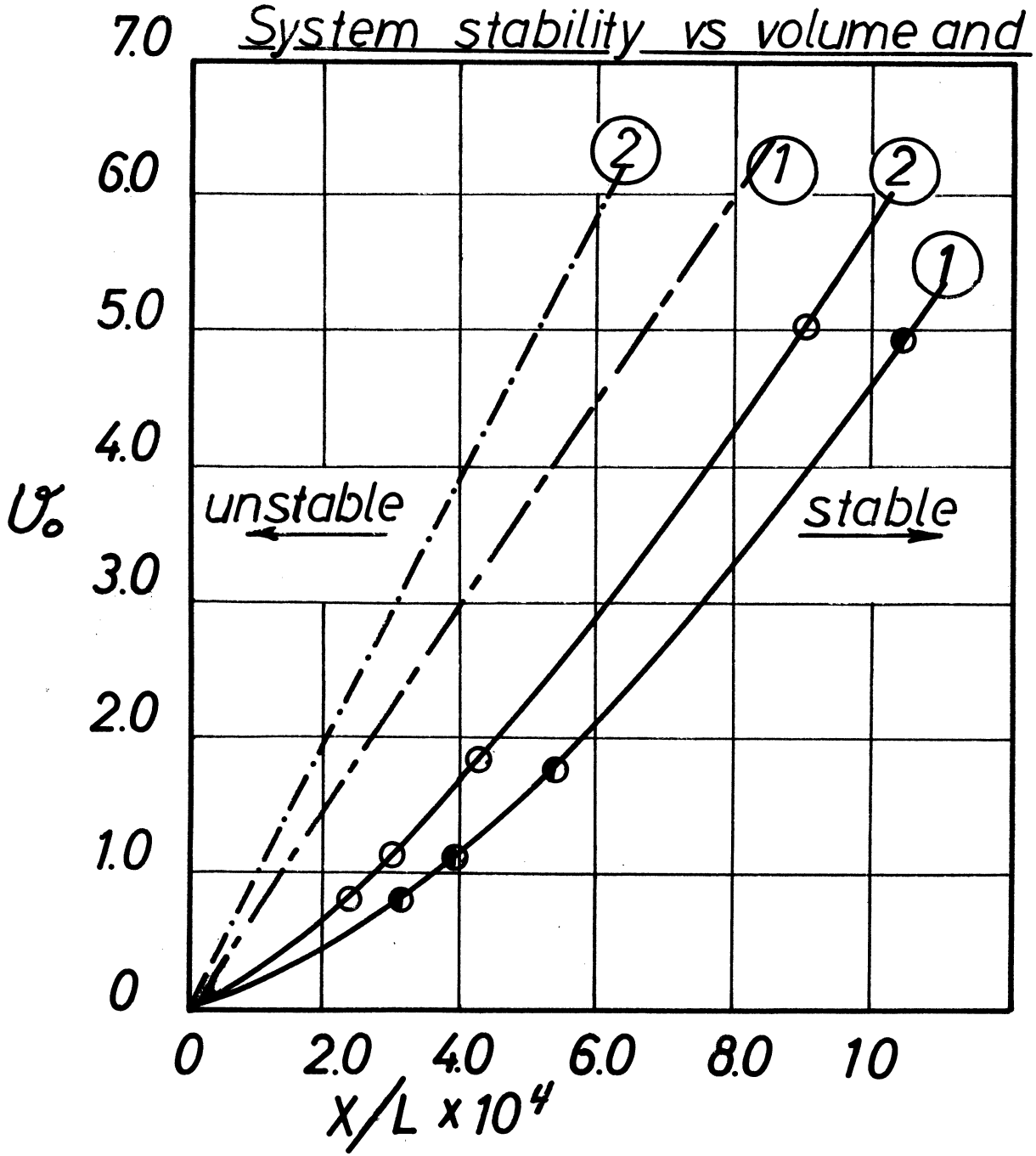

Stable when:

$$\frac{X}{L} \geq \frac{2\rho P_s}{\beta M} V_o$$

$L = 8.0$ inches

(1) $P_s = 800$ psi

(2) $P_s = 600$ psi

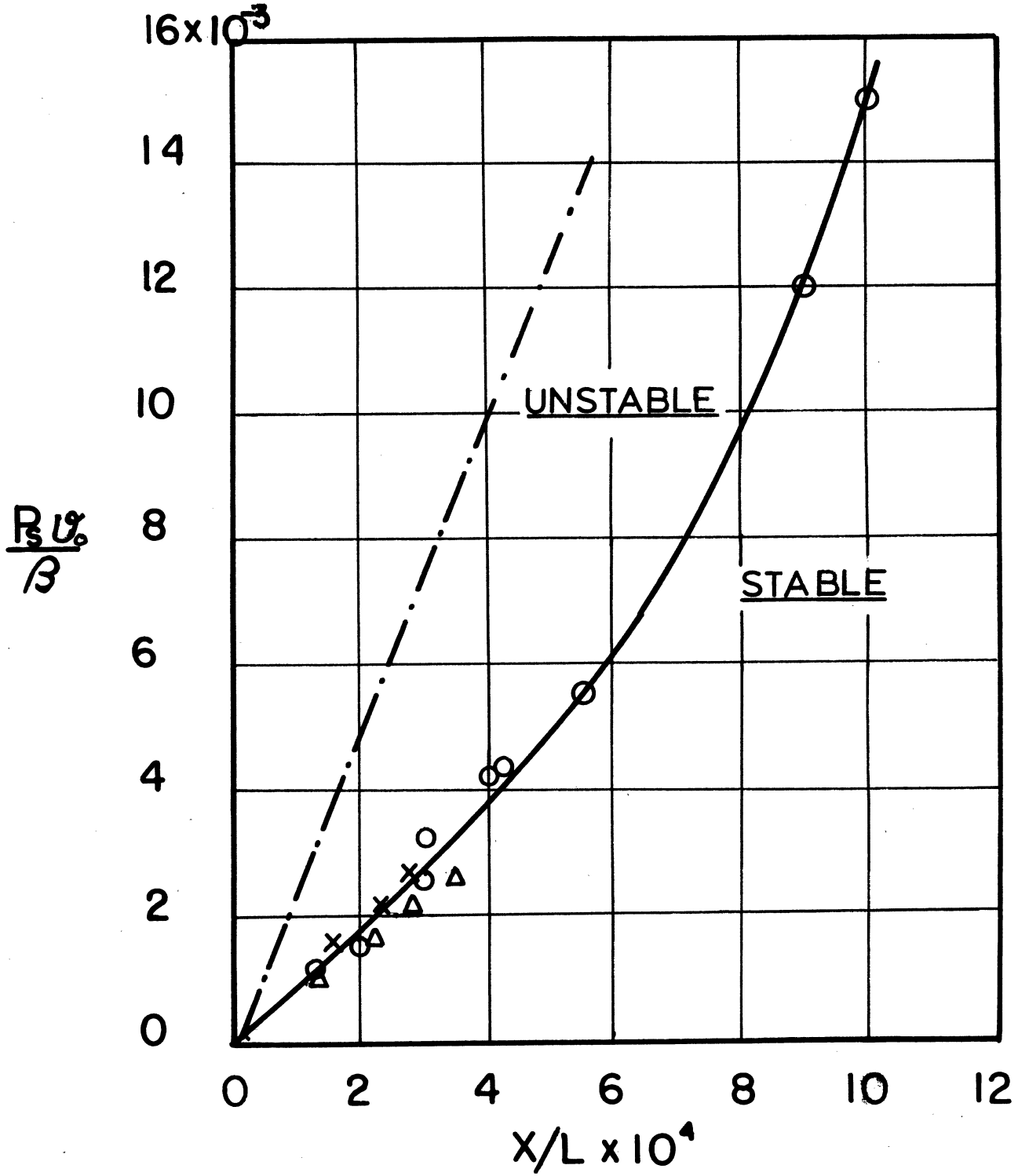

FIGURE 3-12

SYSTEM STABILLITY VS VALVE POSITION

System stable for

$$\frac{X}{L} \geq \left[\frac{2P_s}{\beta}\right]\left[\frac{\rho U_o}{M}\right]$$

O — L = 8 inches vs U_o and P_s

x — L = 8 inches vs P_s

Δ — L = 8 inches vs P_s

·—· Theory for β = 250,000 psi

occurred that were not explained by the theory.

For no external spring applied or very low rates, the poppet would go into slow oscillations. These same oscillations occurred for larger valve displacements or large flows when the valve was restrained by a heavier spring. This seems to tie in with the effect of downstream compressibility as out lined in section 2.20. Since the return line was fitted with a gate valve, the frequency of oscillations could be changed by closing the valve. The downstream piping consisted of elastic hoses which reduced the effective compressibility of the system.

APPENDIX A:

Experimental Apparatus and Procedure

The Apparatus

An apparatus was designed and tested by Taft Murray (Ref.#9) as part of a Masters Thesis project. This same apparatus was used in this investigation with some modifications.

The schematic of the apparatus is shown in Figure A-1.

The apparatus consists of three major units: the nozzle, the poppet and the drive assemblies.

The nozzle is a removable unit and can be changed to conform to any upstream condition that one would like to represent.

The poppet assembly includes the poppet and the drive stem. The stem is housed in an air bearing to reduce friction to a minimum.

A compensating chamber is provided, applying a constant force by the air pressure p_B, to compensate for the static hydraulic forces on the poppet. The force gage is an integral part of the stem. This is a semiconductor bridge-type gage with very high stiffness and sensivity.

A linear, variable, differential transformer (L.V.D.T.) position pickup is attached to the stem,

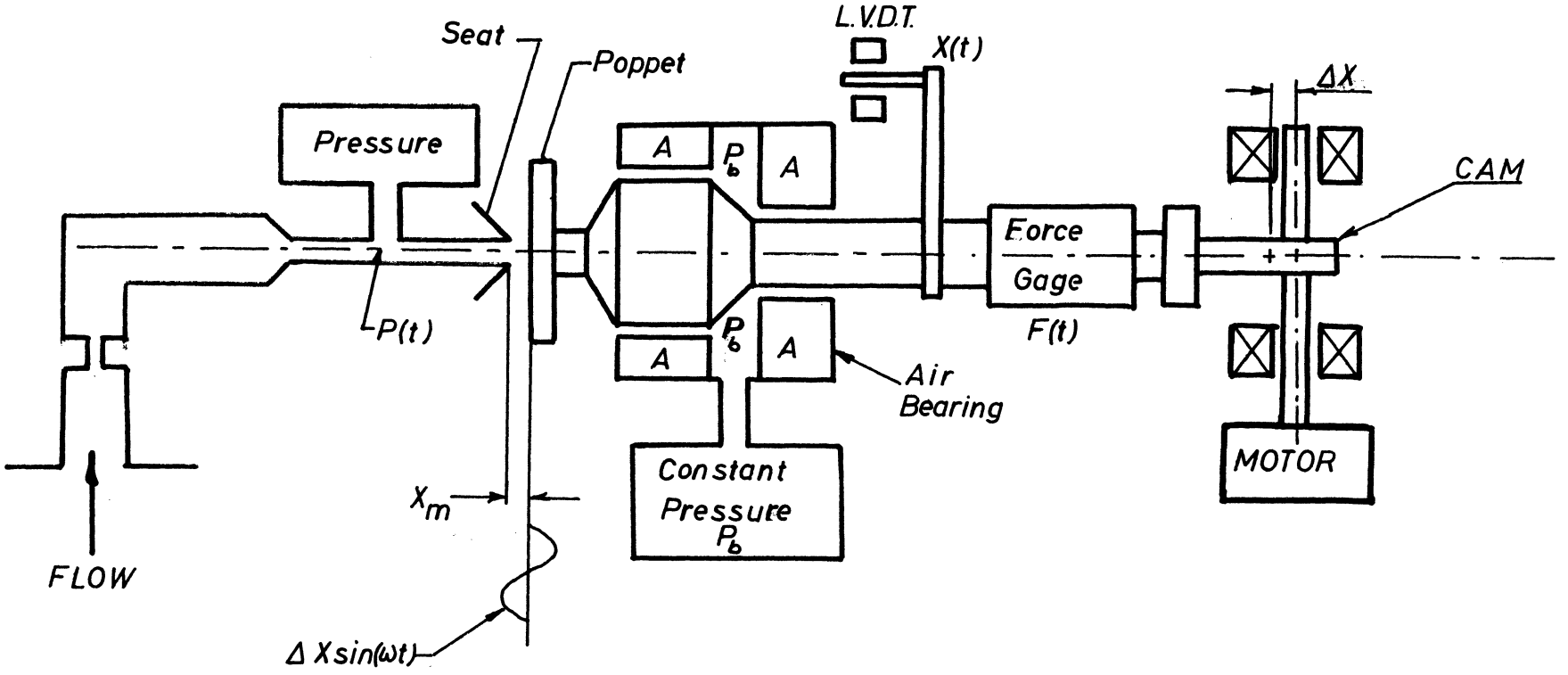

SCHEMATIC OF APPARATUS

to monitor valve displacement.

The drive unit is a sinusoidel cam, provided by grinding the cam surface that holds the cam bearing eccentric to the two main bearings. The cam displacement can be varied by moving the cam bearing in any position between the bearings marked (1) and (2) and is proportional to the distance from bearing (1). Range of eccentricity is .001" to .007". The cam is driven by a variable speed, electric motor with speed range from 3.0 to 45 cycles per second.

The upstream pressure is measured by a pressure transducer, mounted in the nozzle housing immediately upstream of the nozzle.

The electronic instrumentation consists of compensating networks, preamplifiers and a C.E.C recorder. The output signal from each transducer is preamplified, then sent through variable gain and damping compensator network to be recorded on the ballistic CEC Recorder. This gives three simultaneous traces of force, pressure and displacement, and the phase and amplitude relation can be deduced easily.

Calibration:

The calibration was performed as follows.

The pressure sensitivity of the pressure transducer

was checked against a dead weight tester for a 6 volt input to the gage, and the gain set so as to give a galvanometer deflection of 500 psi/in.

The force gage was calibrated by applying a known force of 5 lbs. At 22.5 volts excitation, the output was adjusted to give deflection of 5 lbs/in.

The LVDT transducer was checked against a dial indicator to yield a sensitivity of .002"/in of galvanometer travel.

These calibrations were done at each set of runs as the output of all these transducers is proportional to the excitation voltage.

Procedure for Obtaining P and F vs x.

The procedure here was straight-forward. The apparatus had provisions for changing the upstream parameters L, $\mathcal{V}_o$ and the valve displacement. The upstream orifices were fixed, but changable.

For a given set of conditions the hydraulic test stand was started along with the variable speed motor. Data was recorded at speed increments both for increasing and decreasing speeds, and dwelling long enough at each speed to assure "steady" (uniform) conditions.

Procedure for Checking Stability

To test the stability of the poppet valve, the senusoided drive was removed and a canfilevered spring was attached between the end of the poppet stem and one of the bearing supports. The spring rate can be varied by changing the ratio of length to thickness of the spring.

The dynamic response of the poppet and spring was checked out and the poppet displacement displayed on an oscilloscope.

By plucking the poppet, the natural frequency and damping could be determined.

The damping ratio of the system with no hydraulic pressure on was from .03-.05, so the assumption made in the theory that $c \approx 0$ is good. The natural frequency compared well with that calculated.

To determine the stability for any given upstream configuration, a constant force F_o was applied to the poppet to compensate for the steady-state hydraulic force by the constant air pressure p_B.

The poppet position was then changed through out the range of interest each time it was plucked (representing a step input), and if the initial oscillation died out, the system was stable; otherwise it was deemed

unstable. At times it was not even necessary to touch the poppet to check its stability. Even though this method seems crude, with a bit of feel for it, it yields consistent results.

APPENDIX B-1

Linearization Techniques

Orifice and Valve Flow Equations

Consider the flow through a variable orifice in an incompressible flow. The flow rate Q (in^3/sec) is then given by

$$Q = C A_v \sqrt{\frac{2}{\rho}(P_1 - P_2)} \qquad \text{(B-1)}$$

where:

C = orifice flow coefficient

$A_v = c_o x$ orifice area (in^2)

ρ = fluid density

p_1 and p_2 are the upstream and downstream fluid pressures in (psi)

The linearized form of equation B-1 is arrived at by considering the small changes in flow around some operating point given by the valve displacement x_o. Since flow is a function of both pressure and area we write the change in flow as

$$\Delta Q = K_1 \Delta x + K_2 \Delta P \qquad \text{(B-2)}$$

where K_1 and K_2 are constants. These constants is evaluated as follows. Mathematically, A-1 is of the form.

$$Q = f(X, P) \tag{B-3}$$

and the total change in flow given by

$$dQ = \frac{\partial Q}{\partial X}\Big)_P dx + \frac{\partial Q}{\partial P}\Big)_x dP \tag{B-4}$$

By comparison with B-2 this gives:

$$K_1 = \frac{\partial Q}{\partial X}\Big)_P \tag{B-5}$$

$$K_2 = \frac{\partial Q}{\partial X}\Big)_x \tag{B-6}$$

where K_1 and K_2 are evaluated at the operating point. An example of this technique will be given. Consider the flow from a constant pressure source through fixed orifice A_u and a valve (Ref. Figure 2-1) where the constant pressure is p_s, the intermediate pressure is p and the exhaust pressure is arbitrarily set to zero. From the continuity equations we get for the intermediate pressure

$$\frac{P}{P_s} = \frac{1}{1 + \gamma^2} \tag{B-7}$$

where

$$\gamma = \frac{A_v}{A_u} \tag{B-8}$$

The linearized flow for the upstream orifice from equation B-2 is

$$\Delta Q_u = K_3 \Delta P \tag{B-9}$$

From A-6 we obtain, by differentiation,

$$K_3 = -\frac{C A_u \sqrt{2/\rho}}{2\sqrt{P_s - P}} = -\frac{Q_o}{2(P_s - P)} = \frac{Q_o}{2P_s(1 - \frac{P}{P_s})} \tag{B-10}$$

but the use of B-7 gives:

$$K_3 = -\frac{Q_o}{2P_s}\left[\frac{1+\gamma^2}{\gamma^2}\right] \tag{B-11}$$

Equations B-9 and B-11 now describe the flow through the fixed orifice at any operating point of the valve.

For the variable downstream valve the flow is:

$$\Delta Q_v = K_1 X + K_2 \Delta P \tag{B-12}$$

Equation B-5, upon differentiation, gives

$$K_1 = \frac{Q_o}{X} \tag{B-13}$$

and B-6 with B-7 yields

$$K_2 = \frac{Q_o}{2P_s}(1+\gamma^2) \qquad \text{(B-14)}$$

APPENDIX B-2

Dynamics of a Line

The dynamical equation of incompressible, frictionless, flow for a line will be developed here. Consider a section of a pipe as shown in Figure C-1a. The two sections are spaced a differential length apart and the properties at each section differ only by differential amounts. By applying Newton's equation of motion we have.

$$PA-(P+dp)(A+dA)=\rho(A+\frac{dA}{2})dx\frac{dV}{dt} \qquad \text{(B-15)}$$

Dropping differentials of higher order yields

$$d(pA)=\rho A\frac{dV}{dt}dx \qquad \text{(B-16)}$$

This is the differential equation of motion for a line of variable crossection.

For a line of constant area A and length L, equation B-16 becomes, when intergrated,

$$P_1-P_2=\rho L\frac{dV}{dt} \qquad \text{(B-17)}$$

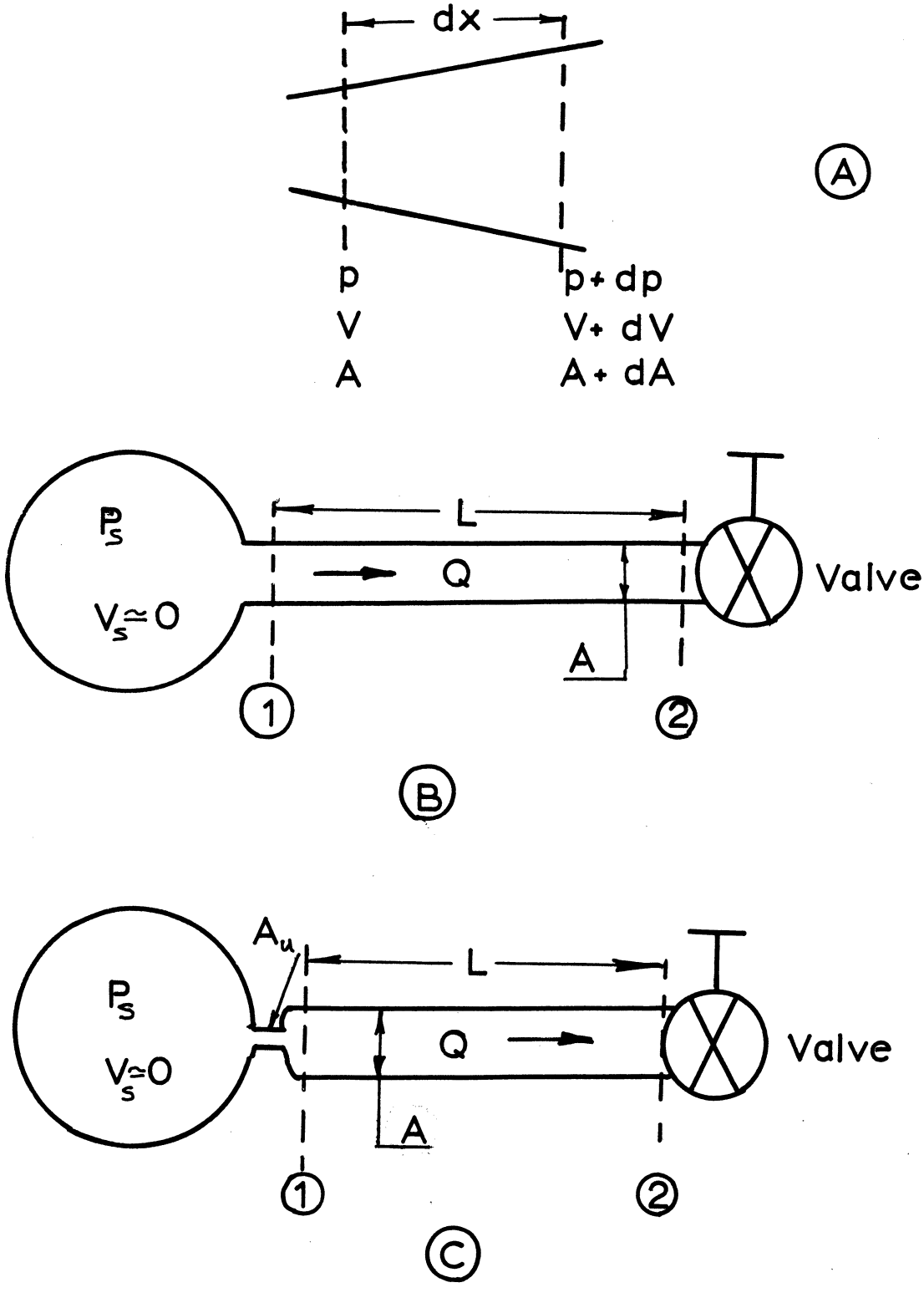

DYNAMICS OF A LINE

FIGURE B-1

P_1 and P_2 are the pressure drops across the pipe, and V is the flow velocity. Substituting the flow rate, $Q = VA$, in equation B-17 gives:

$$P_1 - P_2 = \frac{\rho L}{A}\frac{dQ}{dt} \qquad \text{(B-18)}$$

Equation B-18 is the basic differential equation for a line of constant area and length L

This equation will be used in two cases shown in Figures B-1 b and c.

In Figure B-1 b is shown a constant pressure source connected to the line L and terminated by the valve. We seek the relation between the flow and pressure upstream of the valve (Section 2).

Fluid flow conditions are assumed uniform at sections 1 and 2, so by combining B-18 and Bernoulli's relation from the reservoir, we have

$$P_3 = P_1 + \frac{\rho Q^2}{2A^2} \qquad \text{(B-19)}$$

$$P_3 - P_2 = \frac{\rho L}{A} DQ + \frac{\rho Q^2}{2A^2} \qquad \text{(B-20)}$$

where

$$D = \frac{d}{dt}$$

Since equation B-20 is nonlinear, we will consider the linearized form given by the small perturbation of the flow around Q_o, the mean flow. By differentiation we have

$$-dp_2 = \frac{\rho L}{A} D(dQ) + \frac{\rho Q_o}{A^2} dQ$$

or, if the differential form is dropped,

$$-p_2 = \left[\frac{\rho L}{A} D + \rho \frac{Q_o}{A^2}\right] Q \qquad \text{(B-21)}$$

where p_2 and Q represents the variation in the variables.

Equation B-21 decribes the desired relation between flow and pressure. Explicit functions for either p or Q can be obtained by writing the appropriate equation for the valve.

The second case is shown in Figure B-1 c, where restrictions have been inserted. The relation for pressure and flow will now be given by the flow equation for the restriction and equation B-18 for the line.

Assume we can write the flow through the restriction as:

$$Q = Kp_1 \qquad \text{(B-22)}$$

where $K = \frac{\partial Q}{\partial P}$, as shown in section B-1. Combined with B-18 this yields

$$p_2 = -\left[\frac{\rho L}{A} D + \frac{1}{K}\right] Q \qquad \text{(B-23)}$$

B-23 gives the relation we seek. This is a more general one, in that we have not specified the restriction to any great extent. K could be due to the entrance loss associated with pipes, an orifice, or also thought of as representing the frictional effects in a pipe on a lumped basis. With the expression for K given by the orifice flow (equation B-6) and by letting the orifice area go to the pipe area A, we get equation B-21.

APPENDIX B-3

Stability and Routh Criteria

The stability conditions for a fourth order differential equation will be derived here. A more detailed derivation is found in Ref. #10 section 14.1a)

The differential equation is:

$$\{a_4 D^4 + a_3 D^3 + a_2 D^2 + a_1 D + a_0\} x = 0 \qquad \text{(B-24)}$$

where

$$D = \frac{d}{dt} \qquad \text{(B-25)}$$

Procedure:

We seek the set of columns

a_4 a_2 a_D

a_3 a_1 0

$$\begin{matrix} b_1 & b_2 & 0 \\ c_1 & 0 & 0 \end{matrix}$$

1)

$$b_1 = -\frac{1}{a_3}\left[a_4 a_1 - a_3 a_2\right] \qquad \text{(B-26)}$$

$$b_2 = -\frac{1}{a_3}\left[a_4 0 - a_3 a_0\right] \qquad \text{(B-27)}$$

2)

$$c_1 = -\frac{1}{b_1}\left[a_3 b_2 - a_1 b_1\right] \qquad \text{(B-28)}$$

The condition for stability is now that all the coefficients in the first column are positive, i.e.,

$$b_1 > 0 \qquad \text{(B-29)}$$

$$c_1 > 1 \qquad \text{(B-30)}$$

For condition B-29 this gives

$$-\frac{1}{b_1}\left|a_4 a_1 - a_3 a_2\right| > 0 \qquad \text{(B-31)}$$

$$a_3 a_2 > a_4 a_1 \qquad \text{(B-32)}$$

For condition B-30:

or

$$a_3 a_2 a_1 > a_3^2 a_0 + a_4 a_1^2 \qquad \text{(B-33)}$$

Now, the necessary and sufficient conditions for stability are that the inequalities of B-32 and 33 are satisfied..

They can be rewritten as

$$a_3 a_2 - a_4 a_1 > 0 \qquad \text{(B-32)}'$$

$$a_3 a_2 - a_4 a_1 > a_3^2 \frac{a_0}{a_1} \qquad \text{(B-33)}'$$

Since we assume that all the coefficients are positive, then the term

$$a_3^2 \frac{a_0}{a_1} > 0 \qquad \text{(B-34)}$$

Thus, if equation **B-33'** is satisfied then **B-32'** is always satisfied. Equation **B-32'** is then redundant and the stability is only concerned with **B-33'** or:

$$a_3 a_2 - a_4 a_1 > a_3^2 \frac{a_0}{a_1} \qquad \text{(B-35)}$$

By simple reduction the stability of a third order

equation is found by setting $a_4 = 0$, so:

$$a_2 a_1 > a_3 a_0 \tag{B-36}$$

along with

$$a_0 > 0 \tag{B-37}$$

APPENDIX B-4

Nonlinear Analog Computer Program

Compressibility Effect

This section deals briefly with a computer-program made for analog (computer) study of non-linear system discussed in section 2.40. The system is shown 2-5A and consists of constant pressure supply p_s and flow Q_s through the upstream orifice A_v. The intermediate volume is V_o, the fluid is described by the compressibility β (psi) and density ρ. The flow out through the poppet valve is Q. p_R, the downstream pressure is constant.

System equations

$$Q_s = A_u \sqrt{\frac{2}{\rho}(P_s - P)} \tag{B-38}$$

$$\rho(Q_s - Q_o) = \frac{\partial}{\partial t}(\rho V_o) \tag{B-39}$$

$$Q = A_v \sqrt{\frac{2}{\rho}(P - P_R)} \tag{B-40}$$

and

$$\rho = \rho_o + \frac{\rho_o}{\beta} P \tag{B-41}$$

By combination, the resulting differential equation is obtained.

$$\frac{V_o}{\beta}\frac{dP}{dt} + A_v \sqrt{\frac{2}{\rho}(P - P_R)} - A_u \sqrt{\frac{2}{\rho}(P_S - P)} = 0 \tag{B-42}$$

In order to study this equation on the computer, we bring it into nondimensional form.

Define:

$$Z = \frac{P}{P_S} \quad \& \quad \gamma = \gamma = \frac{A_v}{A_u} \tag{B-43}$$

Return pressure p_R is small such that $p_R/p_S << 1$

Equation 5 then becomes

$$A\frac{dz}{dt} + \gamma\sqrt{Z} - \sqrt{1-Z} = 0 \tag{B-44}$$

where:

$$A = \frac{V}{\beta A_u}\sqrt{\frac{\rho P_S}{2}} \tag{B-45}$$

Equation is nondimensional except for variables in time. Since the constant A has the dimension of time, one can write:

$$\hat{t} = \frac{t}{A} \tag{B-46}$$

where $\hat{t}$ is the nondimensional time. Then it follows that

$$dt = A d\hat{t} \tag{B-47}$$

which gives upon substitution

$$\dot{Z} + y\sqrt{Z} - \sqrt{1-Z} = 0 \tag{B-48}$$

where $\dot{Z} = \frac{dZ}{d\hat{t}}$

Equation 11 gives the desired differential equation we want to study. y is our input and Z is the system response.

The system in this case was driven sinusoidally, but both step, or ramp inputs response can be studied.

Scaling:

Since the analog computer compares voltages as representing system variables, we must make sure that these signals have same scaling (or units) so as to be consistent when compared. The problem is analogous to that of dimensional analysis in mechanics.

The best example is the term $\sqrt{1-Z}$, and the first question is, how do you represent 1? From the expression

we see that when Z is unity or represented by "one unit of Z", the term is zero. Let us represent Z by e volts/"unit of Z". Substituting this we get

$$\sqrt{1 - e} = 0$$

$\therefore e = 1 \Rightarrow e_o$ volts/unit of Z and are term thus scaling e_o, and is given in relation to the unit representation of $\underline{Z}$. Similar arguments hold for the other terms.

By completing the scaling for each term we can draw the complete schematic computer diagram as used on a Philbrick analog computer. The square root is done on the K5-M units and integration and summation on the K5-u units.

This is shown in Figure B-2.

This program was used on the computer to test out the validity of data obtained both in linear and non-linear operation of the poppet valve. The agreement between computer values and experimental results were good. This substantiates the idea of the computer use in the stability analysis.

ANALOG COMPUTOR PROGRAM

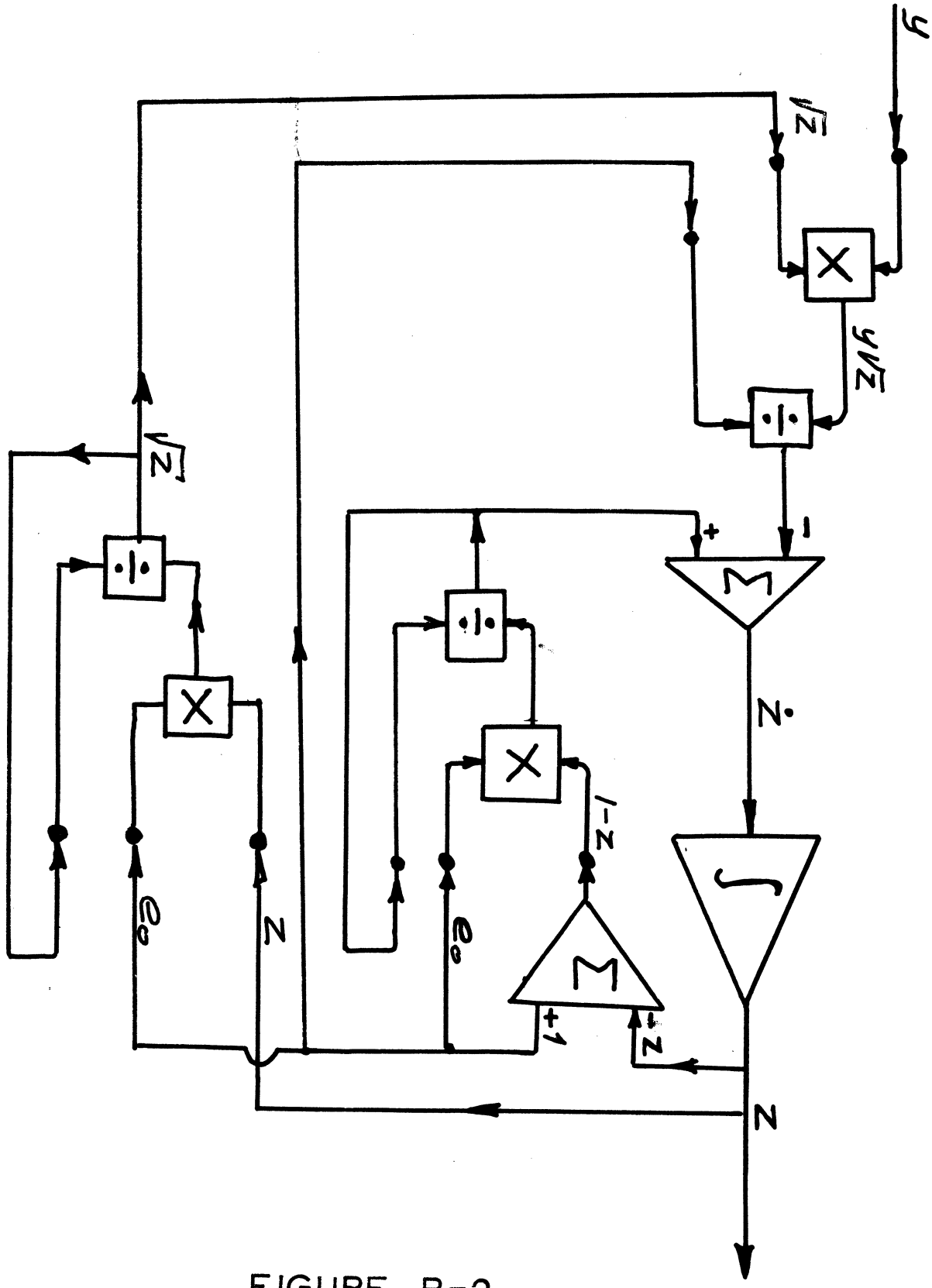

FIGURE B-2

APPENDIX C

Extension of Analysis

Appendix C-1

Inertia Model With Upstream Restriction

In section 2.50, the effect of fluid inertia was considered. The system considered consisted of a constant pressure source, a line and the poppet valve. Introduction of an upstream orifice of area A_u is considered, as shown in Figure 2-1. We assume P_s constant, with incompressible flow.

System equations:

Orifice $$Q_3 = -K_3 P_1 \qquad (C-1)$$

Line $$P - P_1 = -\frac{\rho L}{A} D Q_3 \qquad (C-2)$$

(Reference Appendix B-2)

Poppet $$Q_3 = K_1 X + K_2 P \qquad (C-3)$$

where K_1 and K_2 are defined as in Appendix B-1. By combining, the following transfer function is obtained.

$$\Delta\left(\frac{P}{X}\right) = -\frac{K_1}{K_2 + K_3} \frac{\left[\frac{\rho L K_3}{A} D + 1\right]}{\left[\frac{\rho L K_R}{A} D + 1\right]} \qquad (C-4)$$

and

$$K_R = \frac{K_2 K_3}{K_2 + K_3} \qquad (C-5)$$

Rewrite equation C-4 as:

$$\Delta\left(\frac{P}{X}\right) = -G_4 \frac{\tau_3 D + 1}{\tau_4 D + 1} \qquad \text{(C-6)}$$

The values in equation C-6 are defined by equation C-4. By substitution and rearrangement this yields

$$\tau_3 = \tau_L \left(\frac{\delta}{\gamma}\right)^2 = \tau_L \left(\frac{A_u}{A}\right)^2 \qquad \text{(C-7)}$$

where $\delta = A_u/A$, $\gamma = A_u/A$ and $\frac{\delta}{\gamma} = \frac{A_u}{A}$

$$\tau_4 = \tau_L \left(\frac{\delta^2}{1+\gamma^2}\right) \qquad \text{(C-8)}$$

and finally:

$$\frac{\tau_3}{\tau_4} = 1 + \frac{1}{\gamma^2} \qquad \text{(C-9)}$$

Equation 13 is the desired expression for stability according to equation 52, section 2.52 and since this ratio is always larger than unity, the system is stable.

The gain is given by

$$G_4 = \frac{2R_3\pi D}{A_u}\left(\frac{\gamma}{\gamma^2+1}\right) \qquad \text{(C-10)*}$$

*Ref. Figure 2-12 for similarity of form.

APPENDIX C-2

Combined Effects Configuration

In this section, the two remaining confiugrations shown in Figure 2-9, Section 2.60 will be considered. Model b in Figure 2-6 is considered first.

System Equations:

Orifice $$Q_3 = -K_3 P \qquad \text{(C-11)}$$

Line $$P - P_1 = -\frac{\rho L}{A} D Q_3 \qquad \text{(C-12)}$$

Volume $$Q_3 - Q = \frac{V_0}{\beta} DP \qquad \text{(C-13)}$$

Valve $$Q = K_1 X + K_2 P \qquad \text{(C-14)}$$

By combining, the expression for p vs. x is on the form

$$\Delta\left(\frac{P}{X}\right) = -G_4 \frac{\tau_3 D + 1}{[\tau_c \tau_3 D^2 + (\tau_c + \tau_4) D + 1]} \qquad \text{(C-15)}$$

where

$$G_4 = \frac{K_1}{K_2 + K_3} \qquad \text{(C-16)}$$

$$\tau_3 = \frac{\rho L K_3}{A} \quad ; \quad \tau_4 = \frac{\rho L K_R}{A} \qquad \text{(C-17)}$$

with

$$K_R = \frac{K_2 K_3}{K_2 + K_3} \qquad \text{(C-18)}$$

and

$$\tau_c = \frac{\forall_o}{\beta(K_2+K_3)} \qquad \text{(C-19)}$$

The expressions in equations C-16, C-17, and C-18 are identical with those of the previous section and equation C-19 is identical with equation 34, Section 2.40. These equations are more general in that if $A_u \rightarrow A$, the line area, this solution in the unit represents the solution in Section 2.60.

The stability of the system is related through equation 62, Section 2.61.

Let us now consider the third basic configuration shown on Figure 2-60, Section 2.60 as model C. The basic assumptions are again the same as with the previous model. The only change is that the compressibility and inertia elements have been switched around.

System equations:

Orifice $$Q_s = -K_3 P_1 \qquad \text{(C-20)}$$

Volume $$Q_s - Q = \frac{\forall_o}{\beta} DP_1 \qquad \text{(C-21)}$$

Line $$P - P_1 = -\left[\frac{\rho L}{A} D + \rho \frac{Q_o}{A^2}\right] Q \qquad \text{(C-22)}$$

Valve $$Q = K_1 X + K_2 P \qquad \text{(C-23)}$$

By combining and rearranging the following is obtained

$$-X\left\{\frac{U_o}{\beta}\frac{\rho L}{A}D^2+\left(\frac{U_o}{\beta}\frac{\rho Q_o}{A^2}+K_3\frac{\rho L}{A}\right)D+\left(1+\frac{K_3\rho Q_o}{A^2}\right)\right\}K_1 =$$

$$P\left\{\left(\frac{U_o}{\beta}\frac{K_2\rho L}{A}\right)D^2+\left[\left(1+\frac{K_2\rho Q_o}{A^2}\right)\frac{U_o}{\beta}+\frac{K_2K_3\rho L}{A}\right]D+\left[K_2+K_3+\frac{K_2K_3}{A^2}\rho Q_o\right]\right\} \quad \text{(C-24)}$$

which can more conveniently be written as

$$\Delta\left(\frac{P}{X}\right)=-G_5\,\frac{B_2D^2+B_1D+1}{A_2D^2+A_1D+1} \quad \text{(C-25)}$$

where the coefficients are defined by equation 30.

Remembering that:

$$\tau_L=\frac{LA}{Q}\;;\quad \tau_c'=\frac{U_o}{\beta K_3}\;;\quad \tau_c=\frac{U_o}{\beta(K_2+K_3)}$$

then

$$B_2=\frac{\tau_c'\,\tau_L}{\left(\frac{A}{A_u}\right)^2+1} \quad \text{(C-26)}$$

$$B_1=\frac{\tau_L+\tau_c'}{\left(\frac{A}{A_u}\right)^2+1} \quad \text{(C-27)}$$

and

$$A_2=\frac{\delta^2(\gamma^2+1)\tau_c\tau_L}{(\gamma^2+\delta^2+1)} \quad \text{(C-28)}$$

$$A_1=\frac{\delta^2(\gamma^2+1)}{(\gamma^2+\delta^2+1)}\left\{\left[\left(\frac{A}{A_u}\right)^2+1\right]\tau_c+\frac{\tau_L}{1+\gamma^2}\right\} \quad \text{(C-29)}$$

$$G\cong\frac{2P_3\pi D}{A_u}\,\frac{\gamma^*}{1+\gamma^2} \quad \text{(C-30)}$$

Closure

The analysis has shown that the transfer function for any system combination can be obtained and expressed as function of the basic lead and lag time constants depending on the complexity.

The introduction of an upstream orifice in the inertia model reduced the system time constants as compared to the preceeding model and also reduced the margin of stability. As the upstream orifice can be considered as lumped system resistance, this then shows that restance in general decrease the available system damping.

Introduction of an upstream orifice in the combined case had a similar effect and also increased the complexity of the equations. For model e this lead to a differential equation of higher order than the previous case. Even though this model was the most general the equations are complicated to analyse. Digital or analog computation seems the easiest way to general stability conditions in this case.

APPENDIX D

Flow Coefficients and Constants

The following pages contain the flow coefficient for the upstream orifices and the poppet valve for the case of $\alpha = 90^{\circ}$ and $\alpha = 60^{\circ}$.

The hydraulic oil used is J-43 and its viscosity is given on Figure D-4.

The density used was assumed constant as the temperature during operation was held at approximately 100°F.

$$\rho = .80 \times 10^{-4} \text{ lbs-sec}^2/\text{in}^4$$

which is based upon the assumption that the specific gravity is .85 at 100 degrees F.

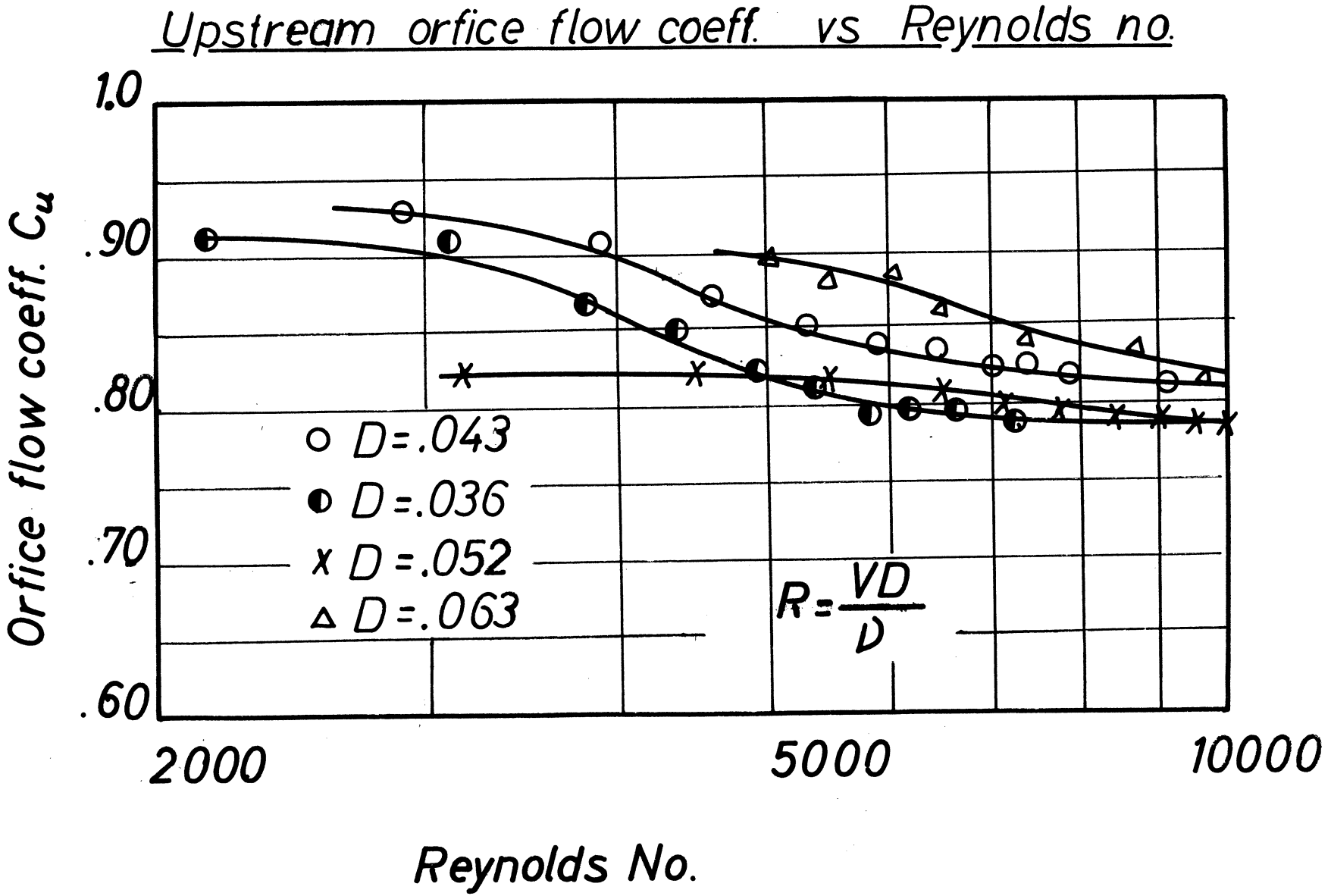
Upstream orfice flow coeff. vs Reynolds no.
1.0
.90
.80
.70
.60
Orfice flow coeff. C_u
○ D=.043
◐ D=.036
x D=.052
△ D=.063
$R=\frac{VD}{\nu}$
2000
5000
10000
Reynolds No.

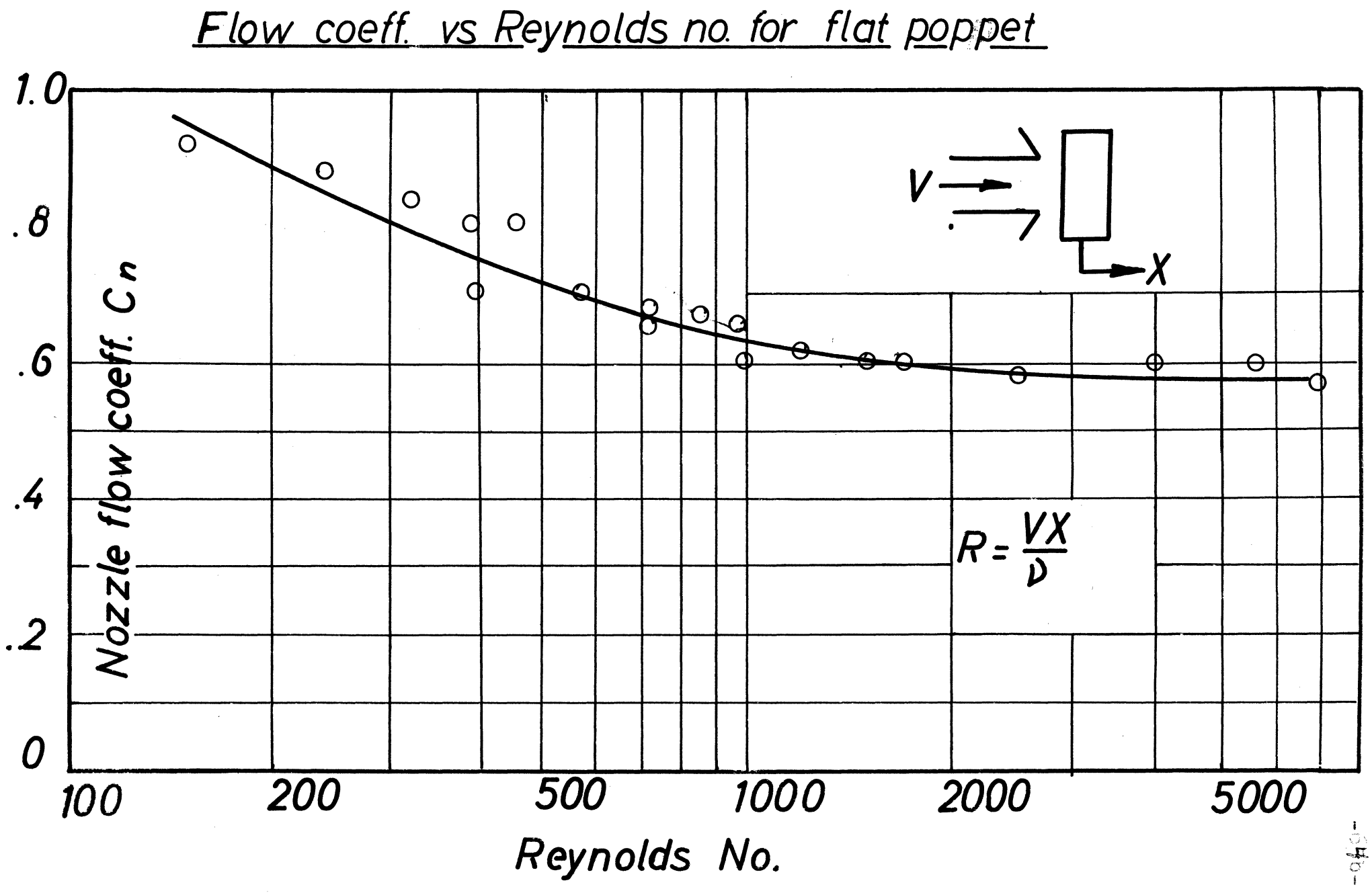
Flow coeff. vs Reynolds no. for flat poppet
1.0
.8
.6
.4
.2
0
Nozzle flow coeff. C_n
V
X
$R = \frac{VX}{\nu}$
100
200
500
1000
2000
5000
Reynolds No.

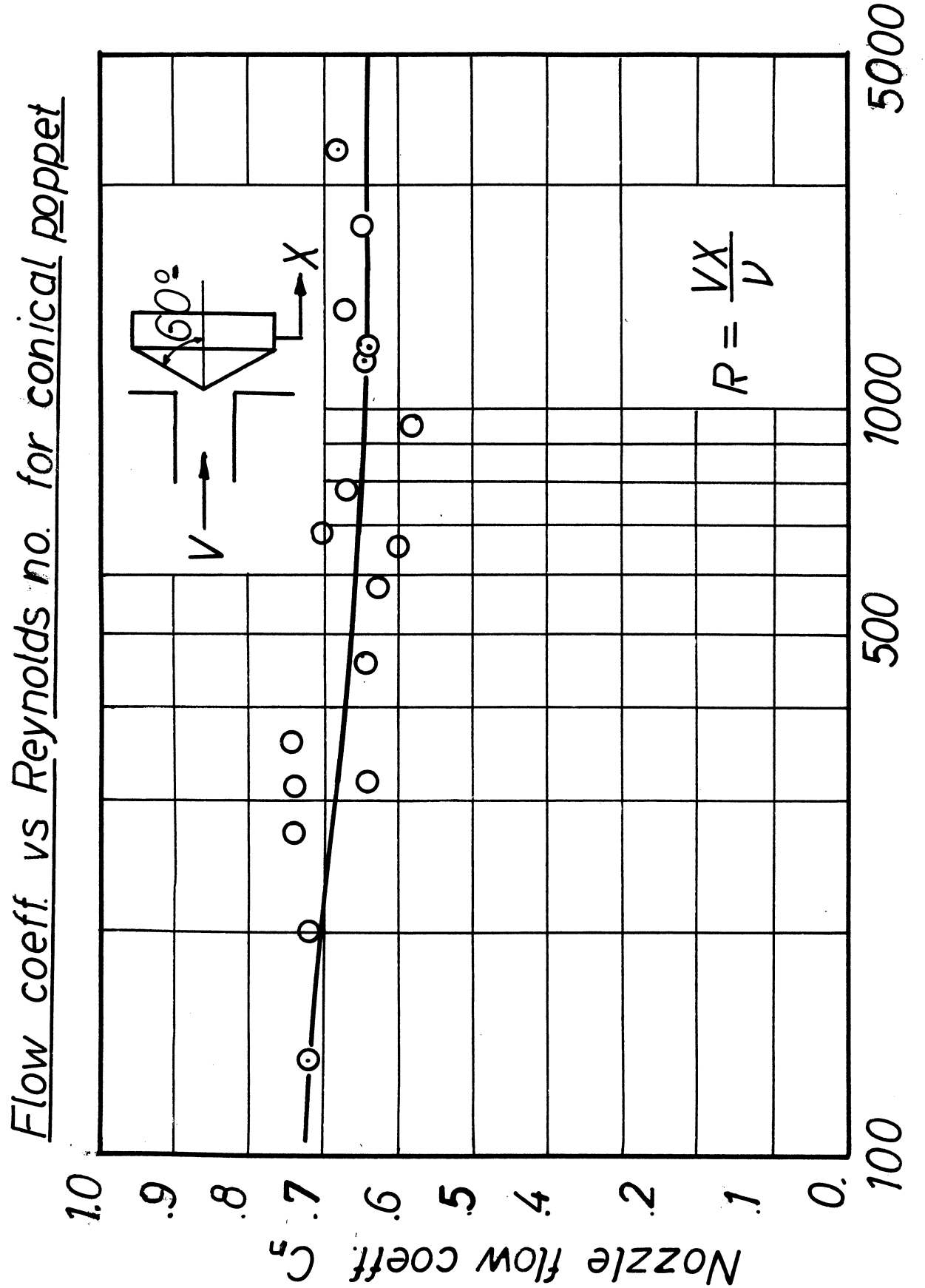
Flow coeff. vs Reynolds no. for conical poppet
Nozzle flow coeff C_n
1.0
.9
.8
.7
.6
.5
.4
.2
.1
0.
100
500
1000
5000
Reynolds No.
$R = \frac{VX}{\nu}$
60°
V
X

VISCOSITY VS. TEMPERATUR FOR HYDRAULIC OIL ; UNIVIS J-43

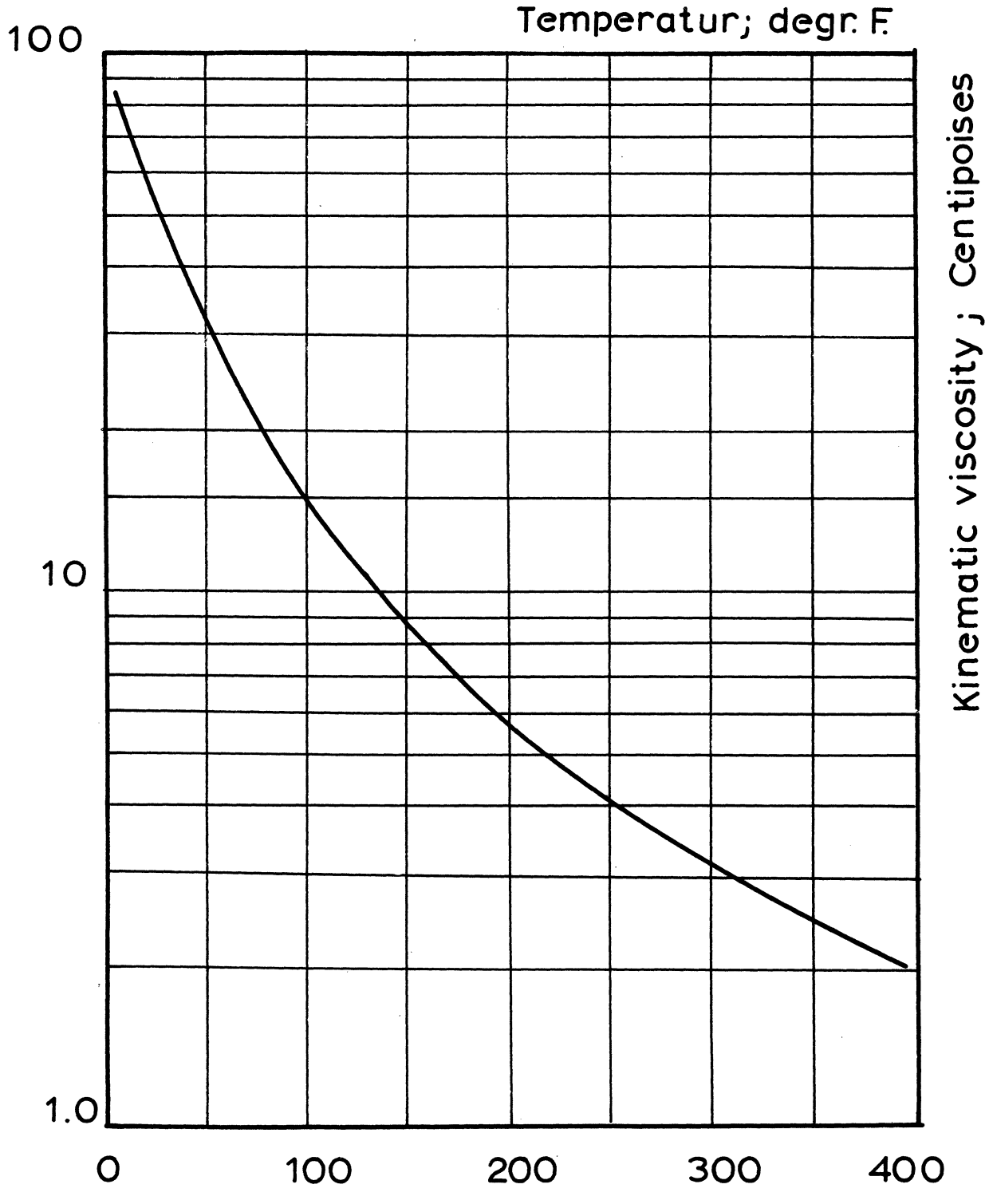

FIGURE D-4

APPENDIX E

List of References

1. Lee, S.Y. and Blackburn, J.F., Axial Forces on Control-Valve Pistons, Dynamic Analysis and Control Laboratory Report M.I.T., June 1950.

2. Stone, J.A., Discharge Coefficients and Steady-State Flow Forces for Hydraulic Poppet Valves ASME, Journal of Basic Engineering Volume 82 , March 1960 (144).

3. Tsai, D.H. and Cassidy, E.C., Dynamic Behavior of a Simple Pneumatic Pressure Reducer, ASME paper 60 WA-186.

4. Feng, T-Y., Static and Dynamic Characteristics of Flapper Nozzle Valves, ASME Transactions Vol. 81, (81).

5. Pawlak, R.J., Stability of a Pneumatic Flapper Valve, Course notes, 2,78, M.E. Dept. M.I.T.

6. Ainsworth, F.W., Effect of Oil-Column Acoustic Resonance on Hydraulic Valve "Squeal", ASME Transactions, May 1953 (773).

7. Funk, J.E., Poppet Valve Stability, ASME paper, 62-WA-160.

8. Freudenreich, J von, The Chattering of Safety Valves and Similar Mechanisms, The Brown Boveri Review, May/June 1948.

9. Murray, F.T., Transient Forces on Hydraulic Seating Type Valve, S.M. Thesis, 1961, M.E. Dept. M.I.T.

10. Fluid Power Control, Blackburn, Reethof and Shearer Ed. Technology Press and John Wiley and Sons, Inc., 1960.